Multi-wavelength Variability and Quasi Periodic Oscillations (QPOs) in Blazars

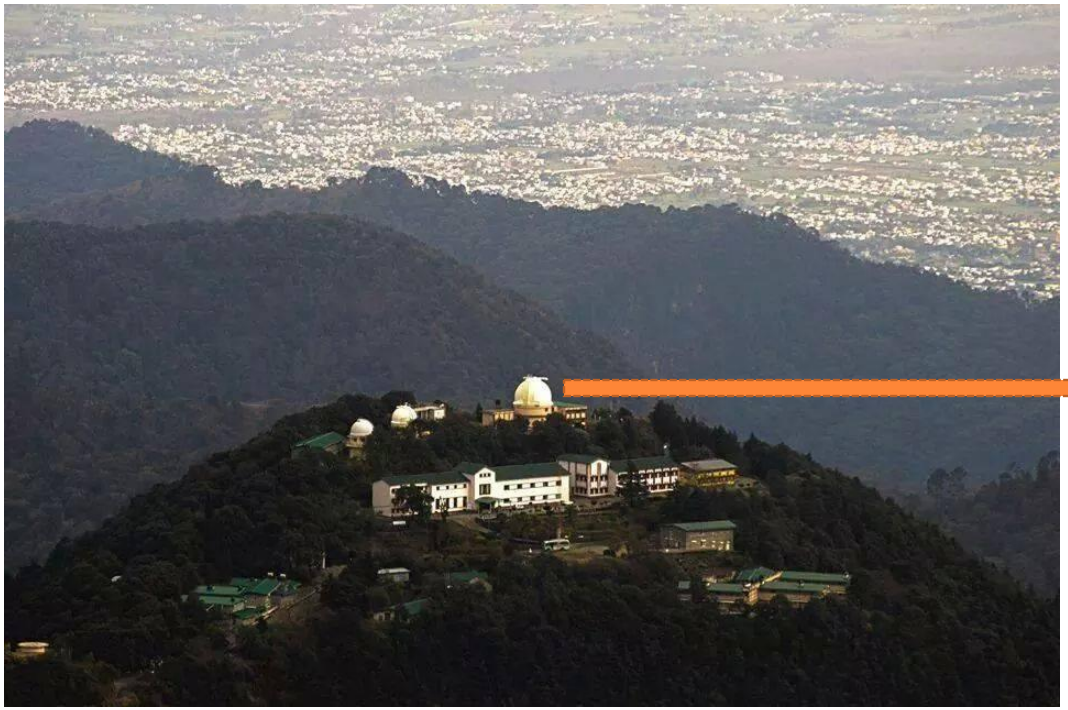

1.04 meter telescope installed in 1972. We have organized a conference to celebrate its 50th Anniversary during 17 – 19 October 2022

Alok C. Gupta, ARIES, Nainital, India
alok@aries.res.in, acgupta30@gmail.com

NAINITAL

Temperature Variation

-5 C to 30 C

3.6m, 1.3m Optical/IR Telescopes and 4m ILMT at Devasthal, ARIES

Time Domain Astronomy and Transient Universe

Explosive Transient Sources

(large range in energies, a time-variable sky**)**

+

Simultaneous Multi-wavelength (MW) Astronomy

↓

Helpful to understand complicated emission mechanism of Transient Sources:

(e.g. GRBs, SN, FRBs, XRBs. UHECRs, **Blazars,** etc.)

Transient Astronomy → MW Variability of Extragalactic Sources

The Transient Universe

Ultra-High Energy Cosmic Rays (UHECRs)

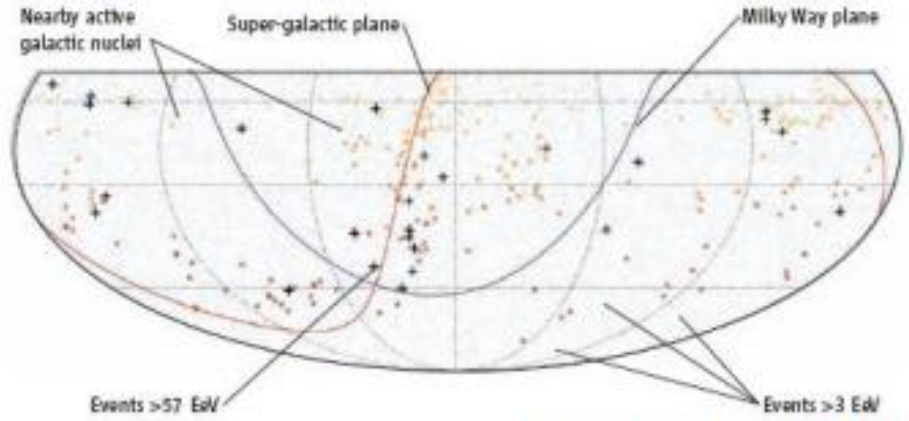

Pierre Auger Collaboration, 2007, Science, 318, 938

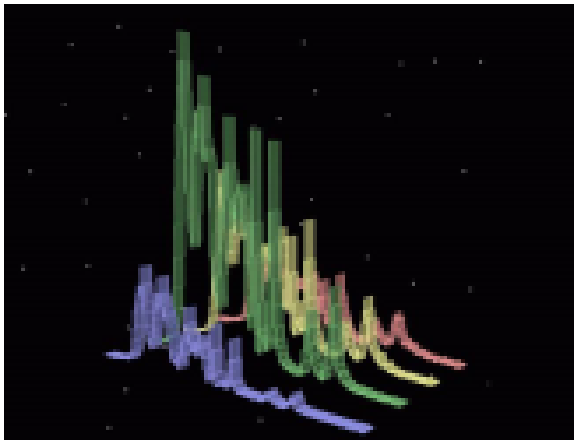

BATSE Catalogue

Gamma-ray bursts

$$\frac{L_\gamma}{L_{EDD}} \sim 10^{10}$$

Radiobursts?

Lorimer et al., 2007, Science, 318, 777

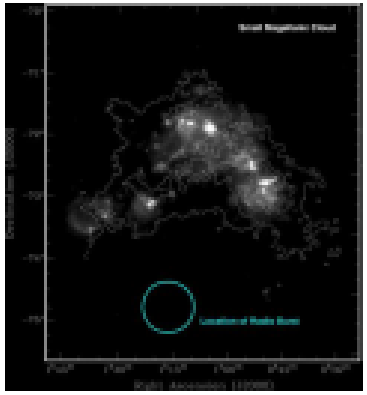

VHE gamma-ray emission is detected from 6 GRBs till date

In last few years studies on **Transient Sources** as producing **Tsunami of Papers**

Revolution in Blazar Studies due to Fermi and recent development in VHE (GeV - TeV) facilities (Fermi-LAT catalogue 2020)

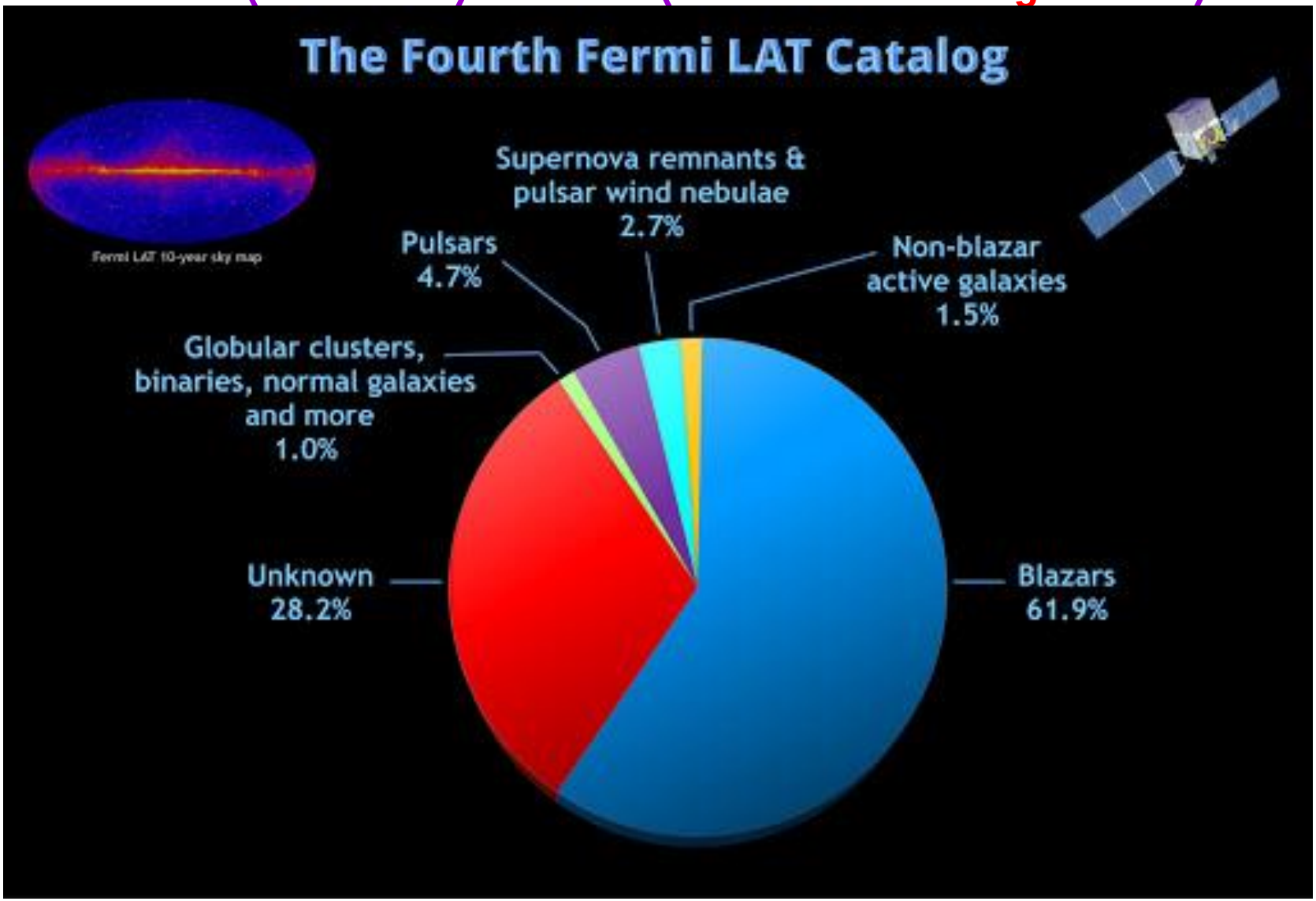

Fermi was launched in June 2008

HESS Telescope in Namibia: 37 institutes, 12 countries and about 200 Scientists + Engineers + PhDs and PDFs → upcoming HESS II, CTA

HESS → High Energy Stereoscopic System

Other similar facilities:

MAGIC (Europe); VERITAS (USA); MACE (India)

Neutrino emission from Blazar TXS 0506+056 (Science 2018)

Till 2005 no. of TeV HBLs known → 6

Till date no. of TeV HBLs known → 78

Blazar (A rare but most powerful class of AGN)

Properties

- ➔ subclass of radio-loud AGN
- ➔ BL Lacs (Featureless optical spectra) + FSRQs (prominent emission lines in optical spectra
- ➔ Variability (in complete EM) on diverse timescales (i.e. IDV, STV, LTV)
- ➔ Variable Polarization radio to optical bands
- ➔ Non-thermal radiation (predominantly)
- ➔ Jet axis angle < 10^0 (Urry & Padovani 1995)

Classification:

- ➔ LBL ↔ RBL (Red ↔ Low Energy ↔ Radio selected)
- ➔ HBL ↔ XBL (Blue ↔ High Energy ↔ X-ray selected)

Spectral Energy Distribution (SED)

SED Peaks

LBL	IR/optical	GeV
HBL	UV/X-rays	TeV

Emission Mechanism

Low Energy ➔ Synchrotron Radiation

High Energy ➔ Inverse Compton (probably)

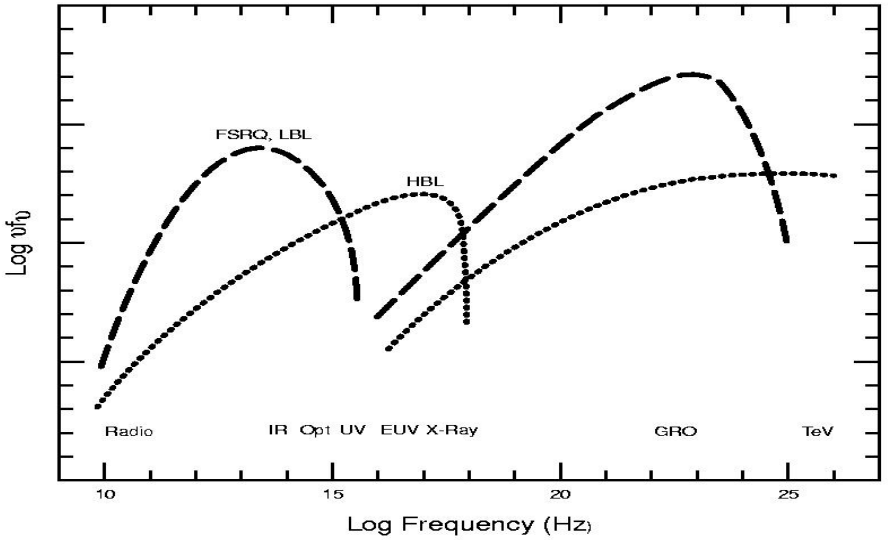

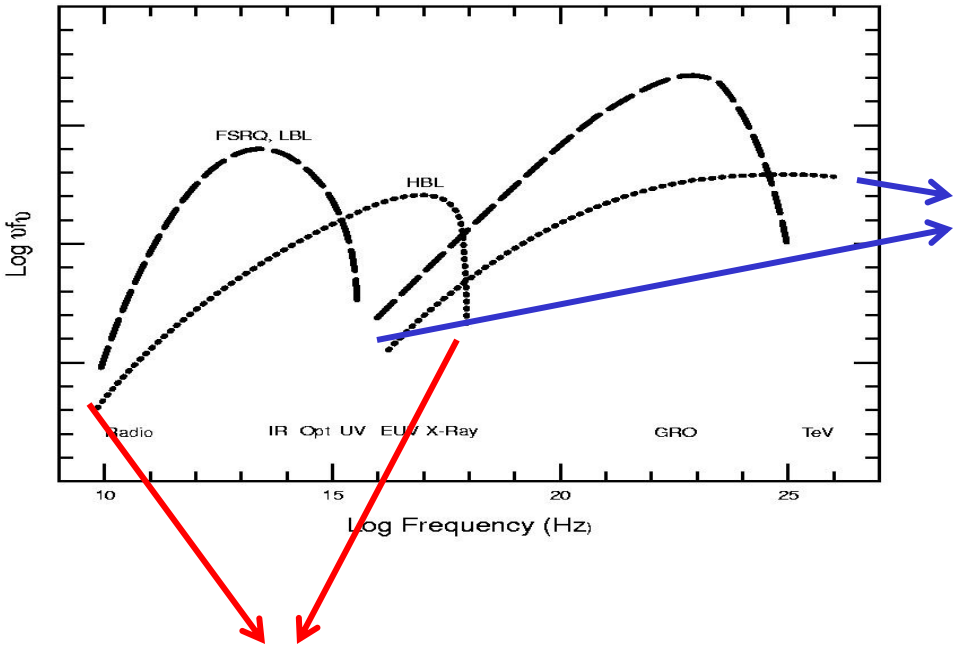

High Energy Part of SED is not well understood. It is usually explained as arising from inverse-Compton (IC) scattering of the same electrons producing the synchrotron emission. These electrons interacts with

1. synchrotron photons → SSC
2. External photons originating in the local environment → EC

Low energy part of SED → well understood

1. Non-thermal Radiation in High State
2. Thermal + Non-thermal Radiation in Low State

Alternative Hadronic Models where Gamma-rays are produced by high energy proton either via proton synchrotron radiation or via secondary emission from photo-pion and photo-pair-production

A lot of challenges to understand high energy part of SED of BLAZARS.

Why to Study Blazars

Blazars are multi-wavelength, and multi-time scale phenomena

Intraday (IDV) – several minutes to less than a day
Short term (STV) – few days to few months
Long term (LTV) – few months to several years

Source of Variability

Intrinsic

- Shock fronts in the jets (IDV and STV)
- Instabilities or hot spots on the accretion disk (variability in the Low-state) (IDV and STV)
- Binary Black Hole Model (LTV)

Extrinsic

- Gravitational Micro-lensing (IDV) **XX**
- It is due to interstellar scintillation and only relevant in low-frequency radio observations. **XX**

Blazar Variability Properties, Time Scales and Physical Implications

Properties	Time Scale	Physical Implications
Irregular & Non-periodic	Few minutes to less than a day (micro or intra-night or intra-day) (IDV)	Size of emitting region, BH mass estimation
Irregular & Non Periodic	One Day to several weeks (short term) (STV)	Useful to search for color variations
Quasi-Periodic	Few months to several years (long term) (LTV)	Useful to predict next Outburst Time, Search for time lag in different energy bands.

Simultaneous multi-wavelength observations of a particular blazar is extremely useful to understand the emission mechanism of blazars and emitting regions in different energy bands.

Hot Spot on/above Accretion Disk

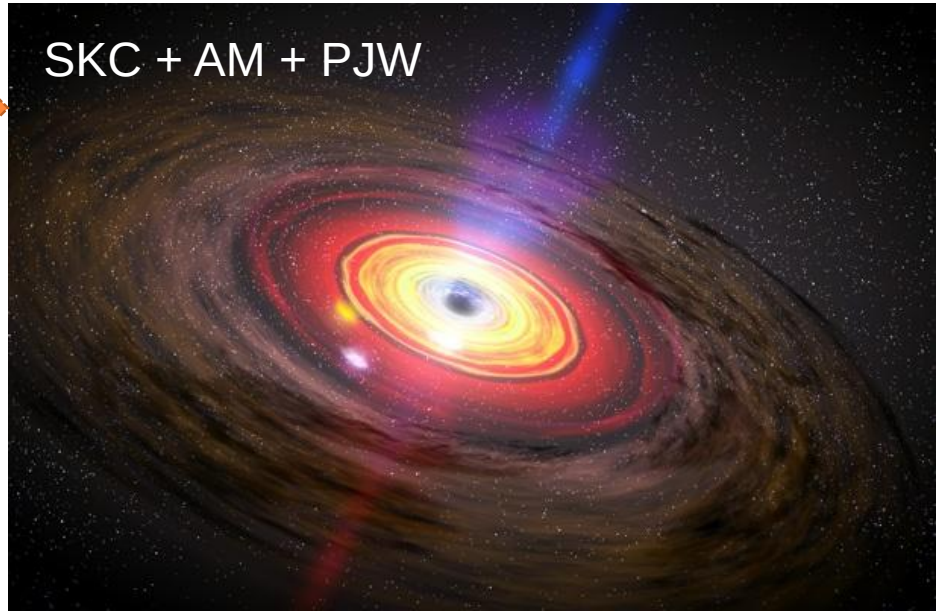

Helical Jet Structure Model

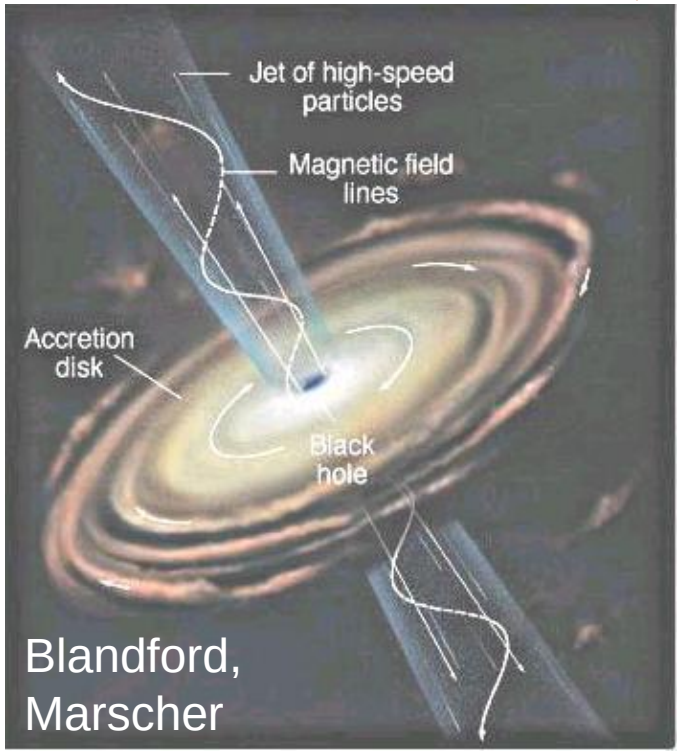

Binary Black Hole Model

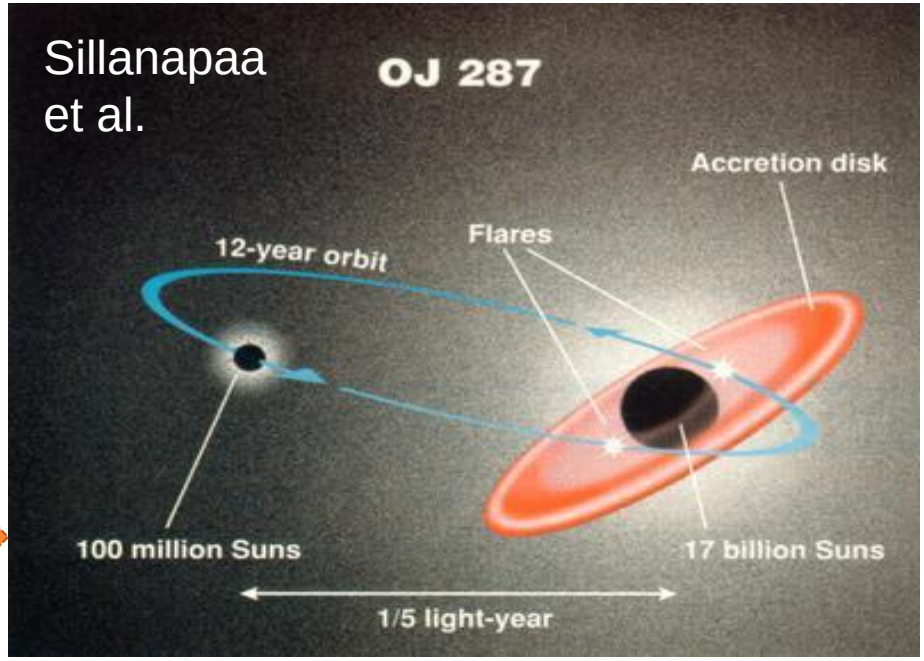

Results and Discussion

Project 1.

Multi-wavelength Variability of Blazars on Diverse Timescales

- Stable Flux
- Decline Flux
- QPO
- Flare

XMM-Newton

- Stable Flux (1a)
- Decline Flux (1b, 3a)
- QPO (2)
- Flare (1c, 3b)

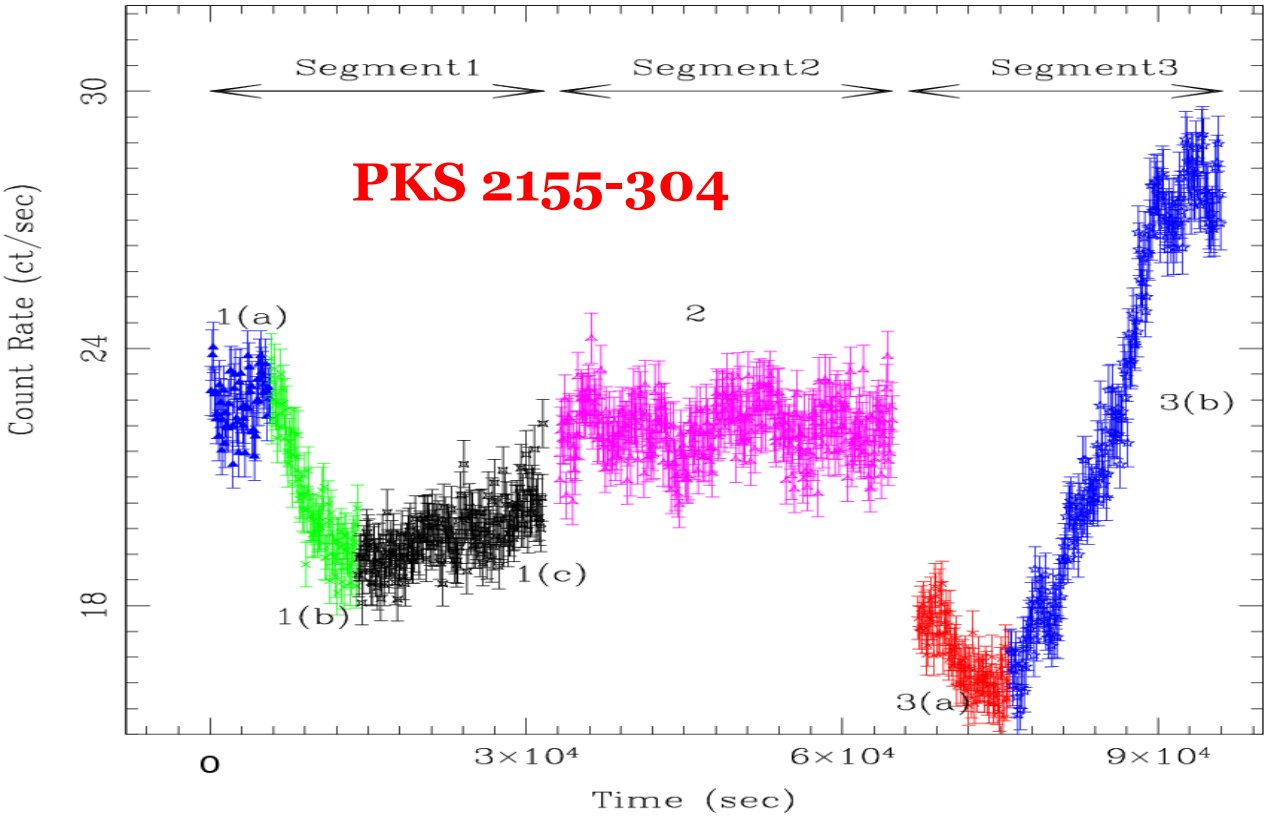

- In sub-segments: 1(a) flux is stable; 1(b) & 3(a) flux decreases; 1(c) & 3(b) show flux rising trend.
- In sub-segment: (2) a hint of weak QPO is detected (Gaur, **Gupta,** et al. 2010, ApJ).
- The percentage variability of segment 1-3 in 0.3 – 10 keV band are 6.6±0.16, 1.5±0.22 and 21±0.15, respectively.

Evidence of jet and accretion disk based models

Bhagwan, **Gupta**, Papadakis, Wiita, 2016

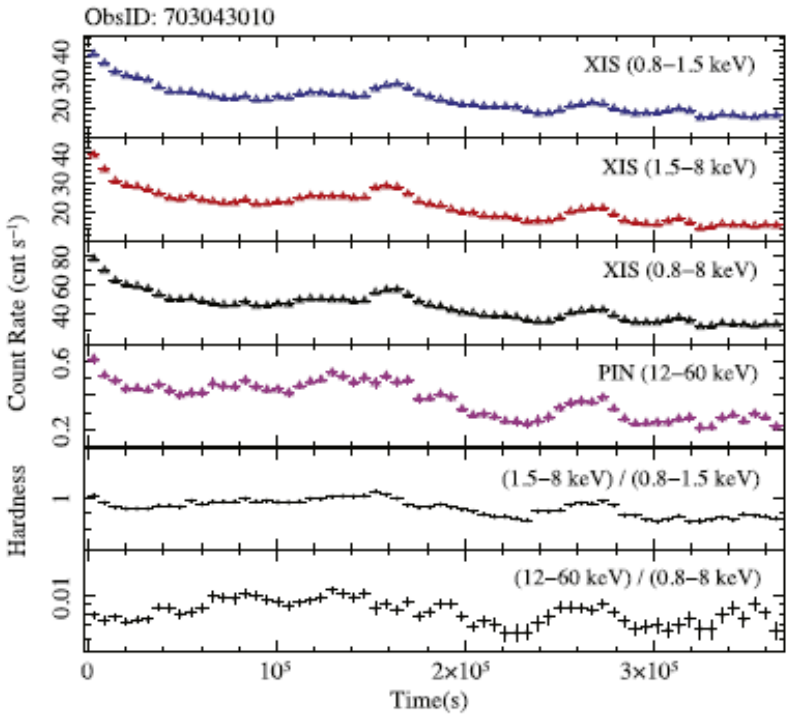

365 ks continuous observation of Mrk 421 with Suzaku

Strong IDV is detected

Soft and Hard light curves are well correlated (DCF peaking at 0 lag).

PSD is red noise dominated.

Nearly similar results we found for about a dozen observations of PKS 2155 – 304 **(Zhang, Gupta, et al. 2021, ApJ).**

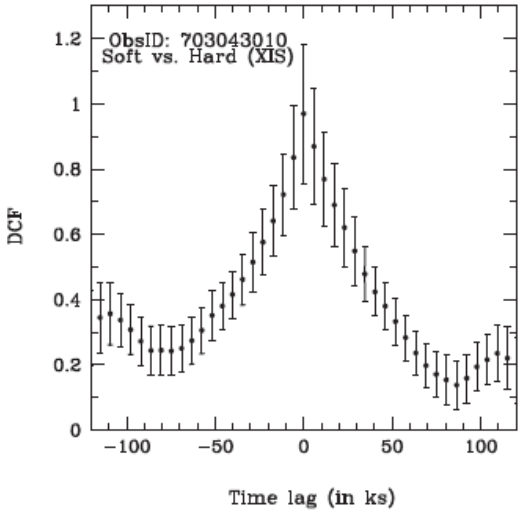

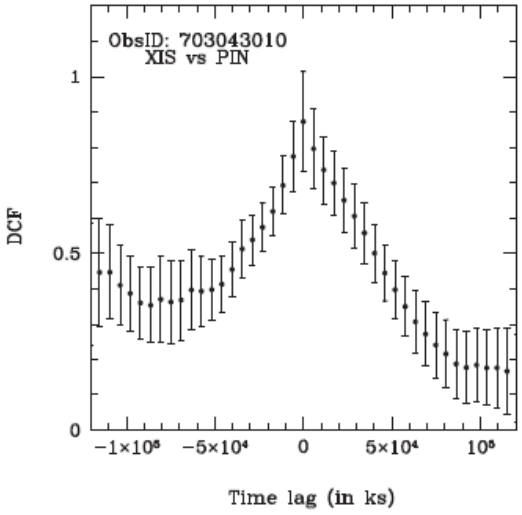

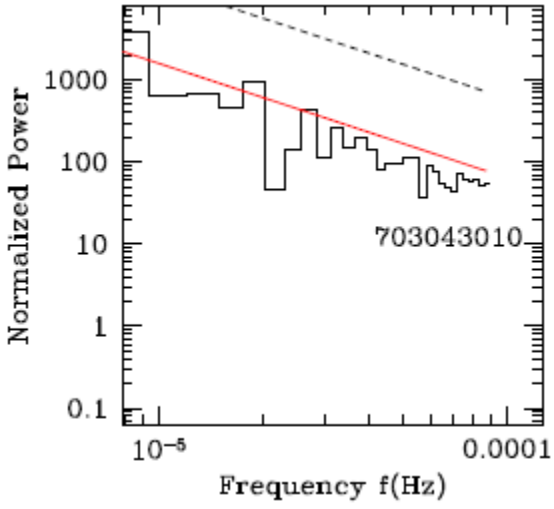

Zhang, Gupta et al. , 2019, ApJ, 884, 125

Intra-day Variability Timescales of TeV Blazars using NuStar and Chandra

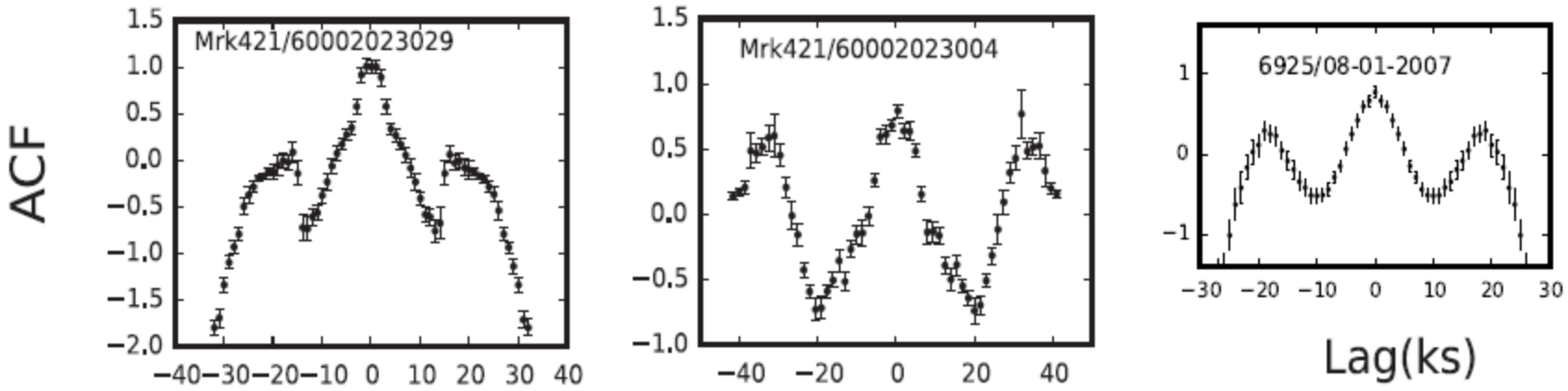

Using intra-day variability timescales, we calculated following parameters of blazars

Model Parameters for *NuSTAR* Blazars

Blazar	t_{var}(s)	δ	B (G)	γ	R (cm)
Mrk 421	2500	25	$\geqslant$0.12	$\leqslant 9.0 \times 10^5$	$\leqslant 1.8 \times 10^{15}$
Mrk 501	8000	15	$\geqslant$0.07	$\leqslant 1.5 \times 10^6$	$\leqslant 3.5 \times 10^{15}$
PKS 2155−304	29600	30	$\geqslant$0.02	$\leqslant 2.0 \times 10^6$	$\leqslant 2.4 \times 10^{16}$

Similar results we found for the Blazar Mrk 421 using Chandra data

Pandey et al. 2017, 2018, ApJ; Aggrawal et al. 2018, MNRAS

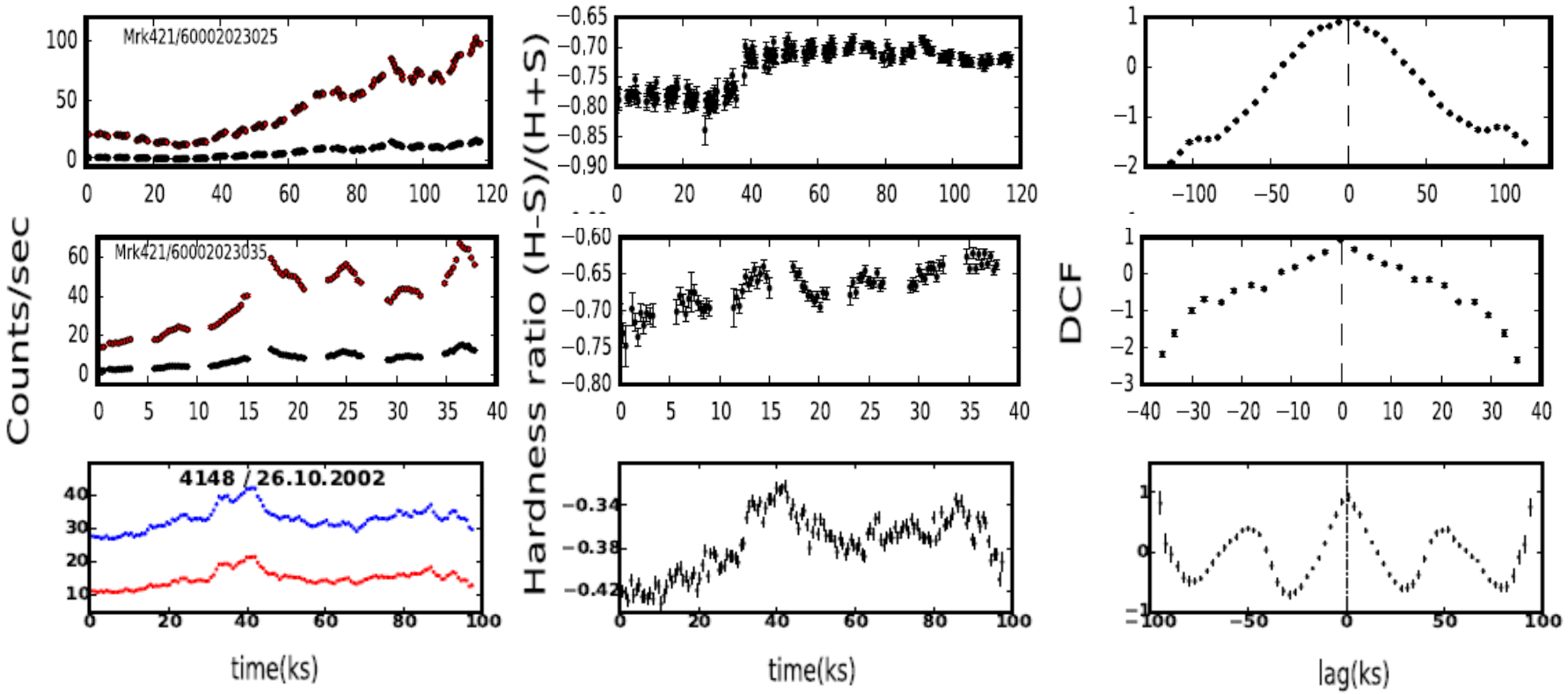

- **In soft (3 – 10 keV) vs hard (10 – 79 keV) using NuStar and soft (0.3 – 2.0 keV and hard (2 – 10 keV) using Chandra, we noticed spectra harden with increasing flux ➔ evidence for harder when brighter.**

- **Soft and hard light curves in NuStar and Chandra are well correlated with zero lag ➔ co spatial emission region by same population of leptons.**

Pandey, Gupta et al. 2017, 2018, ApJ; Aggrawal, Gupta et al. 2018, MNRAS

Long Term Variability of 3C 273 with XMM-Newton

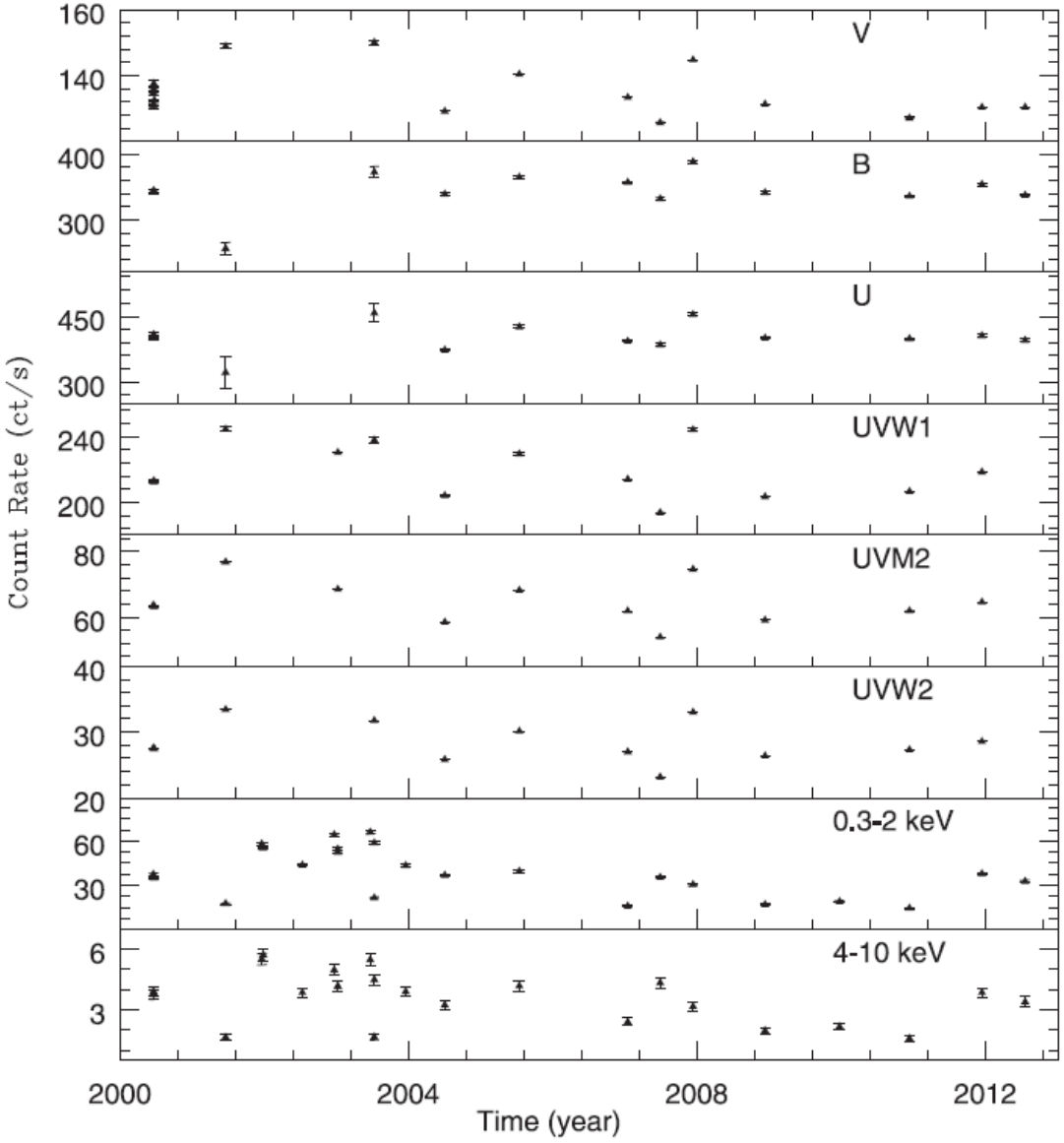

- During the years 2000 – 2012, 3C 273 has 21 observations simultaneously in OM and EPIC-PN.

- We find significant variations, in all bands, on time-scale of years.

- Our visual inspection show that in the long term LCs, optical & UV bands are well correlated and the same is true for hard and soft X-ray bands.

Kalita, **Gupta**, et al., 2015, MNRAS, 451, 1356

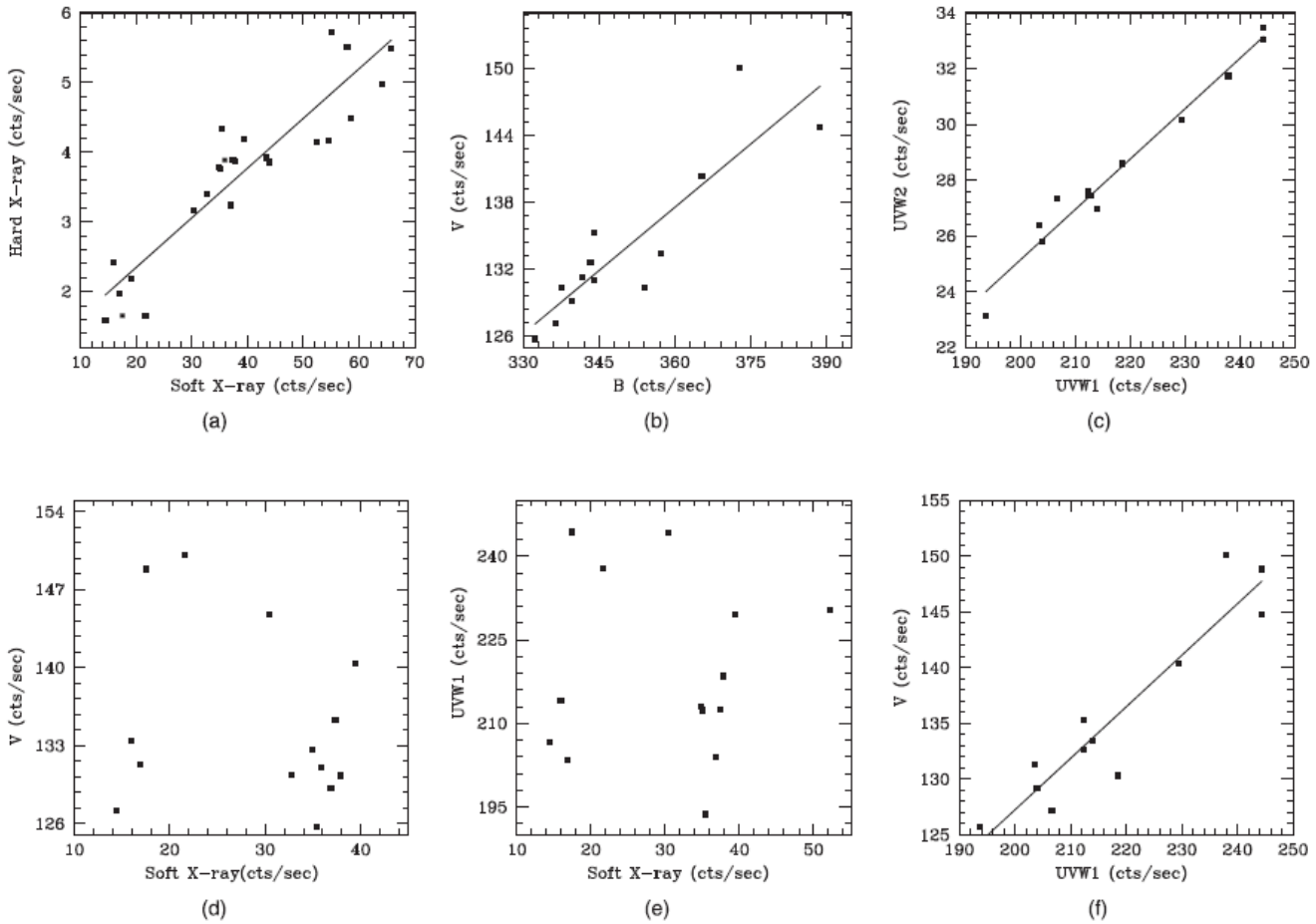

Figure 4. Correlations in variability between different optical, UV and X-ray bands.

Flux Variations in Optical/UV are not correlated with X-rays ➔ Optical/UV emissions in this blazar may arise from different population of leptons.

But optical/UV bands are well correlated, similarly soft and hard X-ray bands are well correlated.

Kalita, **Gupta**, et al., 2015, MNRAS, 451, 1356

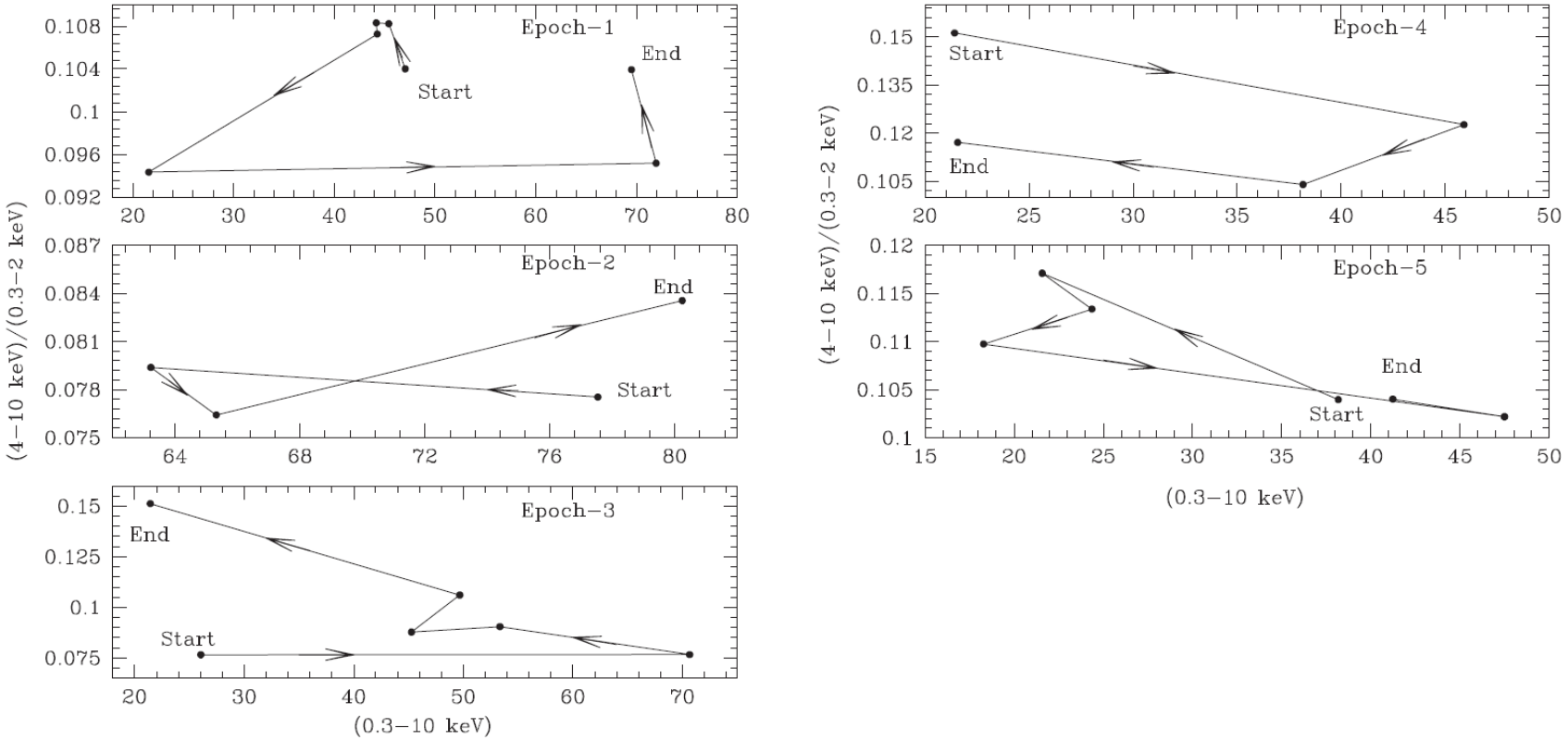

Figure 5. Spectral evolution of 3C 273 in different epochs. Arrows indicate the directions of the loops. Here, the term epoch in the plots represent different time intervals during which the data were acquired for each corresponding loop: Epoch-1 = 13.06.2000–22.12.2001; Epoch-2 = 17.12.2002–18.06.2003; Epoch-3 = 07.07.2003–12.01.2007; Epoch-4 = 12.01.2007– 09.12.2008; Epoch-5 = 06.12.2007–16.07.2012. The clockwise and anti-clockwise loops are distinct and closed or nearly so, presenting a clear evidence of alternate acceleration and cooling mechanism.

In the above HR vs Flux plots, we found clockwise and anti-clockwise loop on different epochs ➔ both synchrotron cooling as well as particle acceleration are at work on different epochs of observations.

Kalita, **Gupta**, et al., 2015, MNRAS, 451, 1356

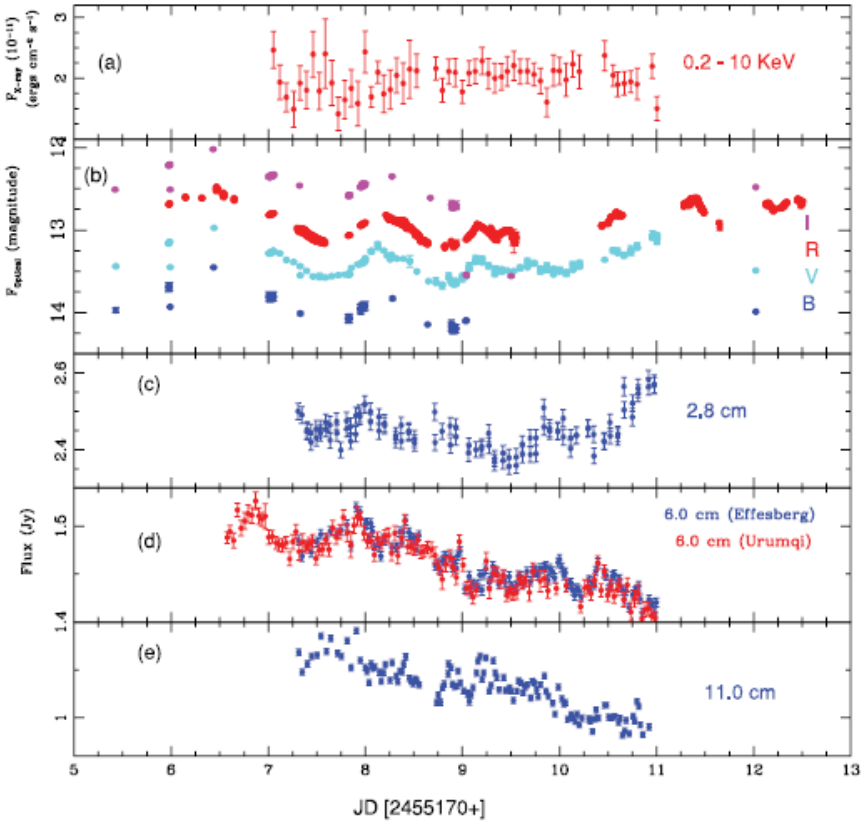

Simultaneous multi-wavelength observations of 0716+714 during Dec 11-15, 2009 (core campaign period).

IDV detected in radio and optical bands.

Total change in optical bands ~ 0.8 mag.

Correlated variability is found in different optical bands.

2.8 cm band data leads 6 and 11 cm bands.

SED was constructed with non simultaneous Fermi data and we got Doppler factor ≥ 12 – 26 which is relatively high for a BL Lac.

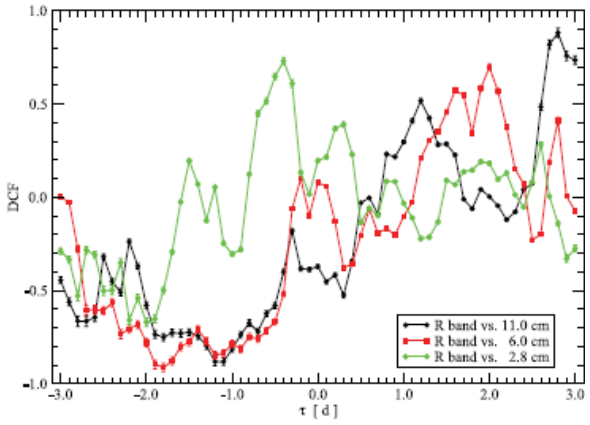

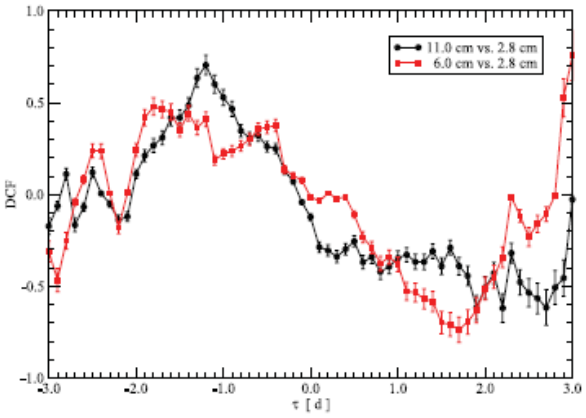

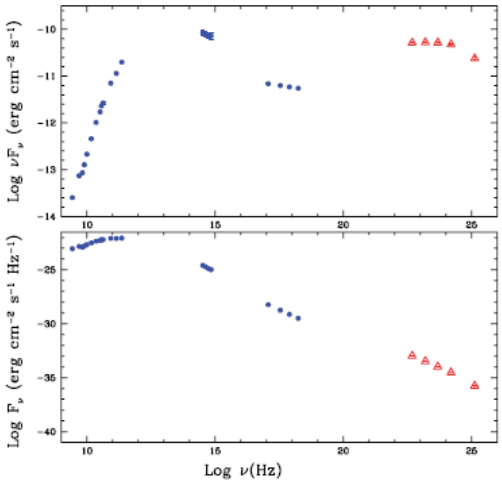

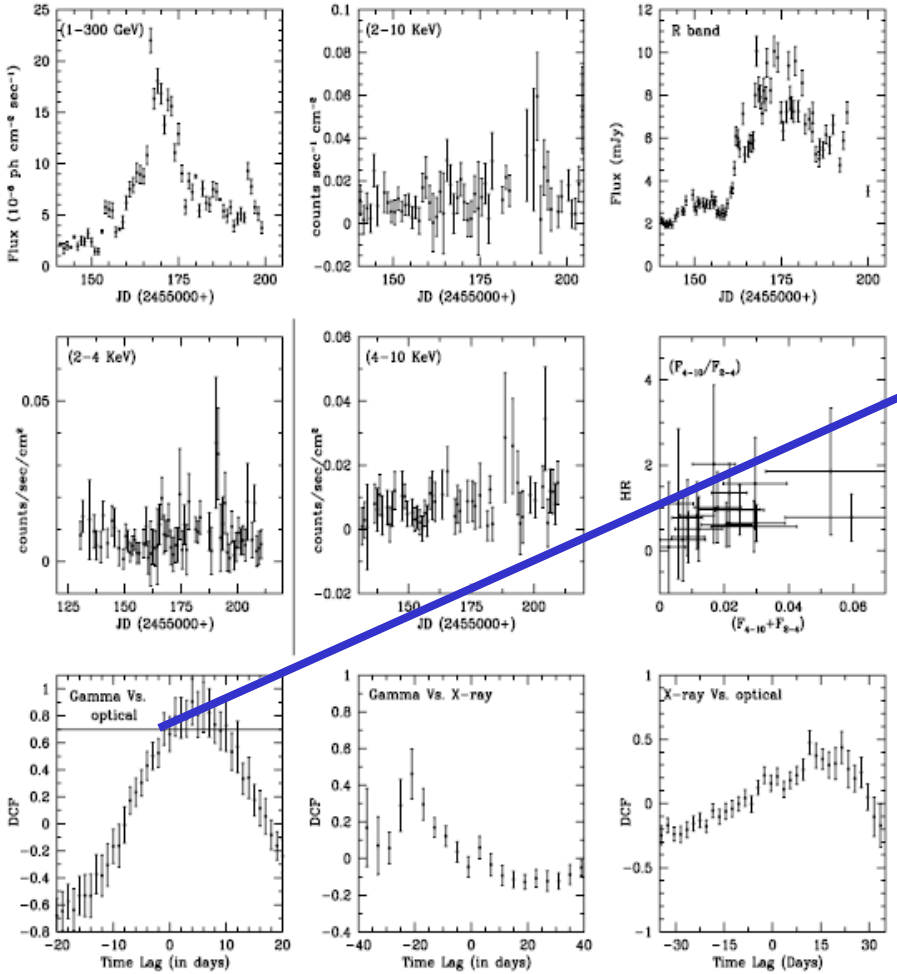

Figure 7. Gamma, X-ray, and optical LCs of 3C 454.3 (upper panels); X-ray LCs for 3C 454.3 in 2–4 keV, 4–10 keV and hardness intensity plot (middle panels); DCF between gamma vs. optical (horizontal line indicates 99% significance level), γ-ray vs. X-ray, and X-ray vs. optical (in lower panels).

3C 454.3

99.9% significance level by using MC simulation.

In the blazar 3C 454.3, we got strong optical and Gamma-ray correlations with time lag of ~ 4 days (gamma-ray leading optical).

External Compton emission mechanism can explain the findings.

Gaur, **Gupta** & Wiita, 2012a, AJ, 143, 23

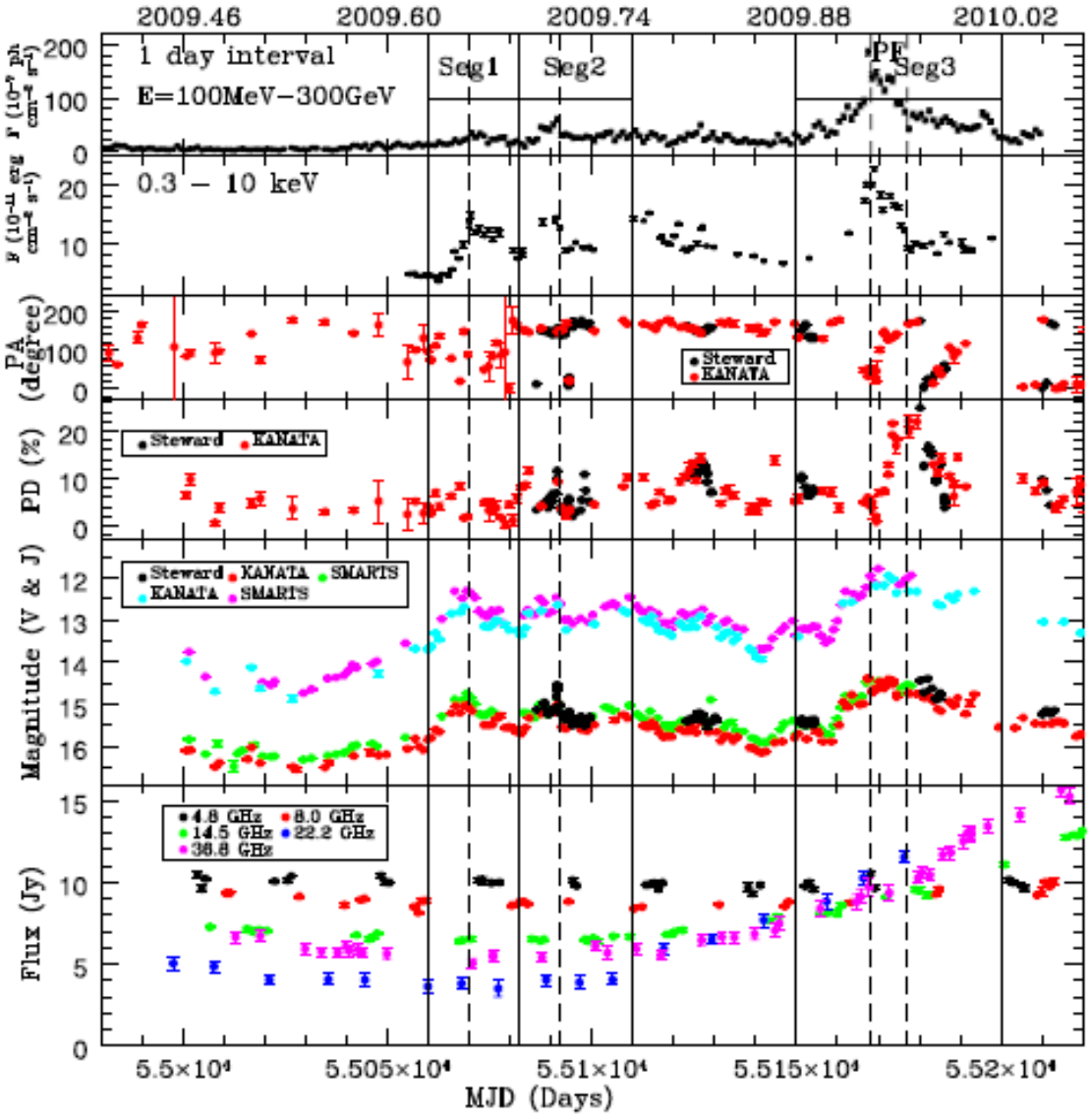

3C 454.3

A strong flare seen in gamma-ray, X-ray and optical/NIR during 2009 December 3-12.

Emission in optical/NIR bands rose more gradually than gamma-rays and X-rays, though all peaked nearly at same time.

Optical polarization showed dramatic change during flare with a strong anti-correlation between optical flux and degree of polarization.

The combination of behavior appears to be unique.

Gupta et al. 2017, MNRAS, **472**, 788

XMM-Newton

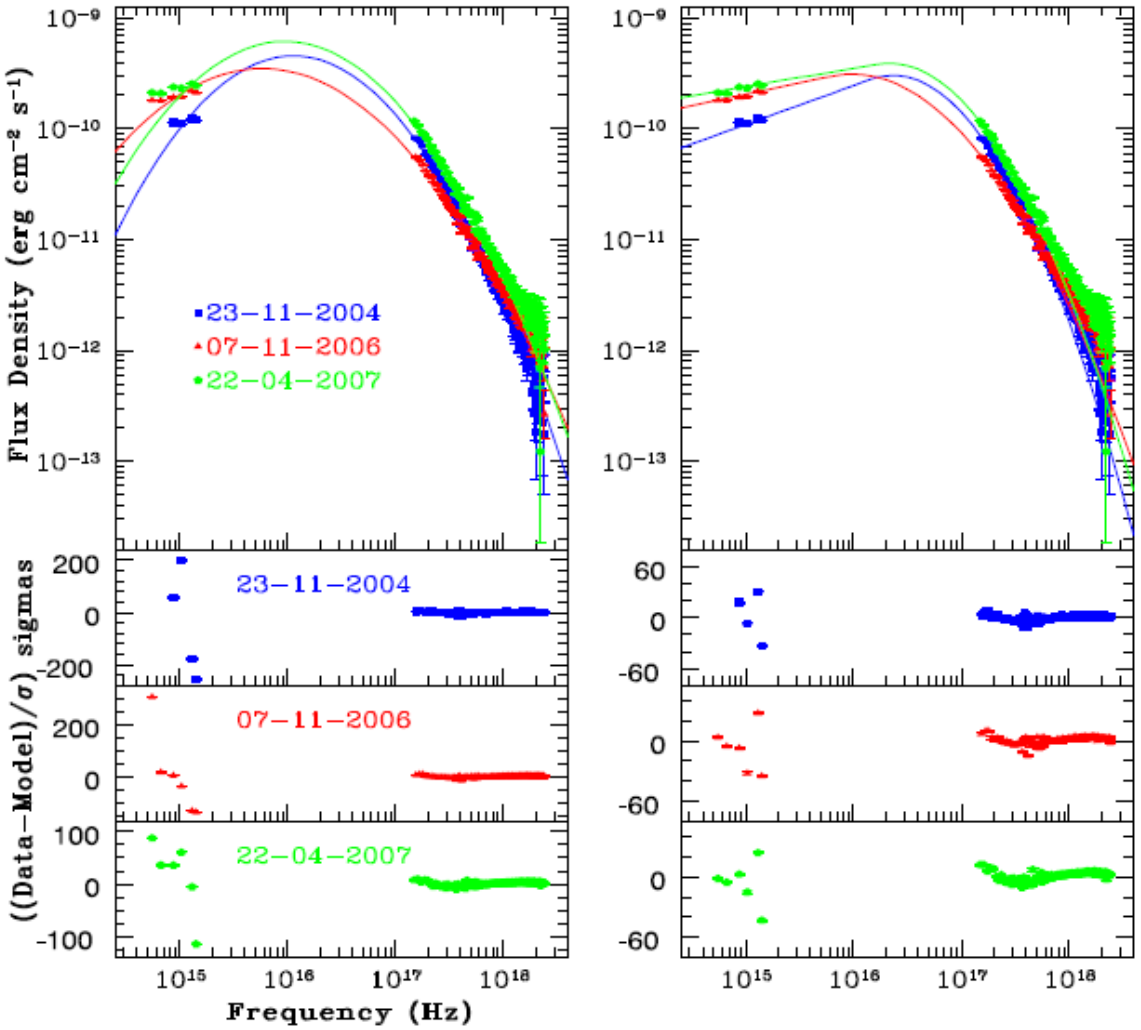

Log Parabolic (LP) Model

Log Parabolic + Power Law (LPPL) Model

- We made the SEDs for all 20 observations which span more than 3 order of magnitude in frequencies.
- We first fitted with log – parabolic (LP) model (left panel). The fits were poor.
- We then fitted with log – parabolic (LP) + Power Law (PL) → (LPPL) model which show significant improvement.
- These models indicate that the optical/UV and X-ray flux variations are mainly driven by model normalization, but the X-ray band flux is also affected by spectral variations, as parameterized with the model curvature parameter.
- The energy at which the emitted power is maximum correlates positively with the total flux. As spectrum shifts to higher frequencies, the spectral curvature increases.

Bhagwan, Gupta, Papadakis, Wiita, 2014, MNRAS, 444, 3647

XMM-Newton

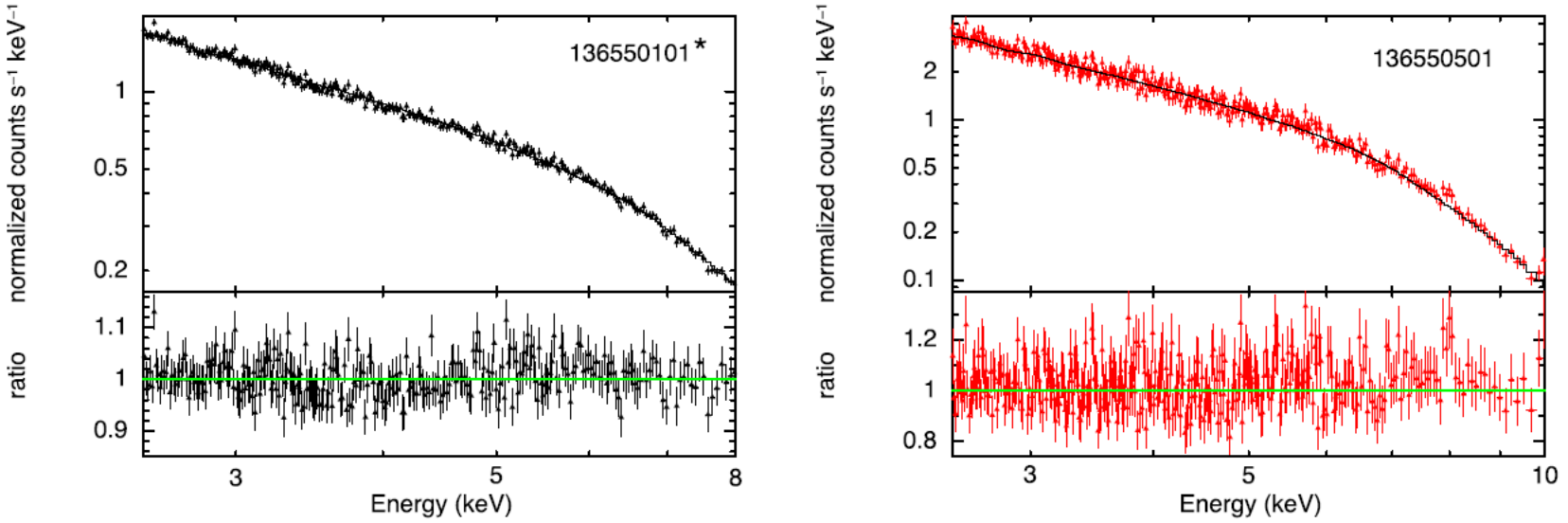

❖ 20 observations of 3C 273 taken during 2000 – 2015. The source was detected in most of the time in low-flux state. A flaring activity in 2007.

❖ Spectra in black (2.5 – 8.0 keV) and red (2.5 – 10 keV). The spectra plotted with asterisk shows pile up.

❖ X-ray spectra is fitted with single power-law model.

Kalita, Gupta, et al., 2017, MNRAS, 469, 3824

XMM-Newton

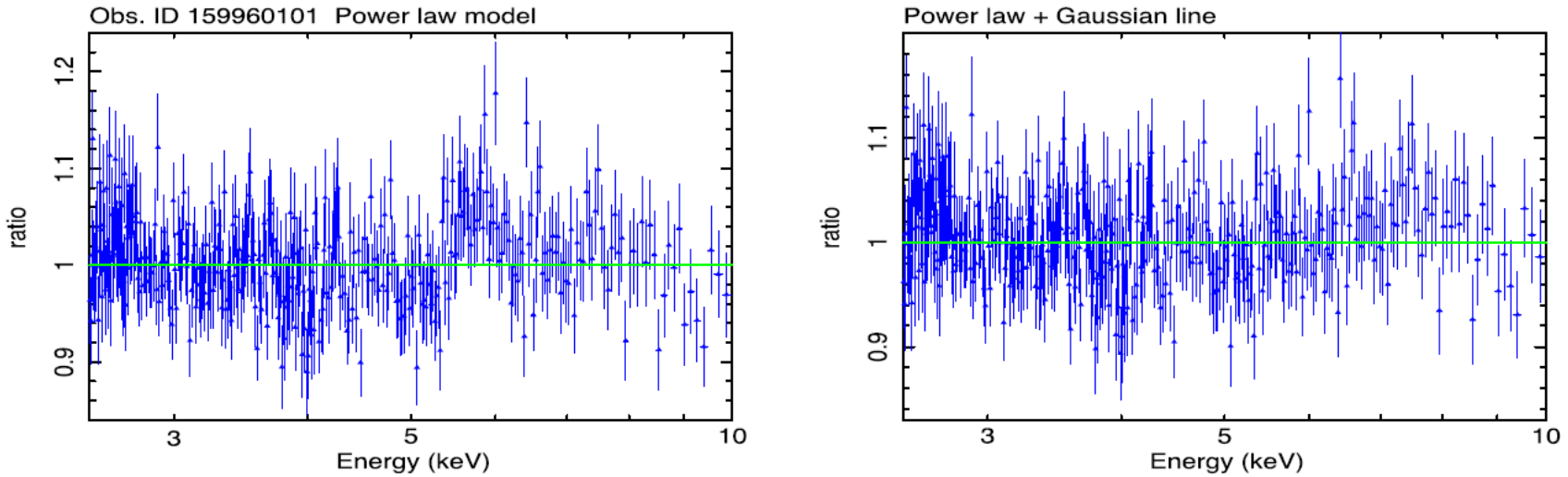

Figure 2. Data-to-model ratios of the observation 0159960101. Left: a simple power-law fit to the spectrum with galactic absorption. At near 6 keV, the residual shows a bump indicating the presence of an iron line. Right: the bump disappears from the residuals after adding a Gaussian line to the power-law spectra; addition of a Gaussian line improves the fit by changing χ_r^2 value from 1.13 to 1.05 ($\Delta\ \chi^2 = 48/3$ degrees of freedom).

Detection of Fe K_alpha line near at its rest energy at 6.4 keV on one observation ID.

Kalita, Gupta, et al., 2017, MNRAS, 469, 3824

Results & Discussion

Project 2.

QPOs in the blazars

Presence of QPOs are fairly common in micro-quasars but rare in AGN

Greiner et al.

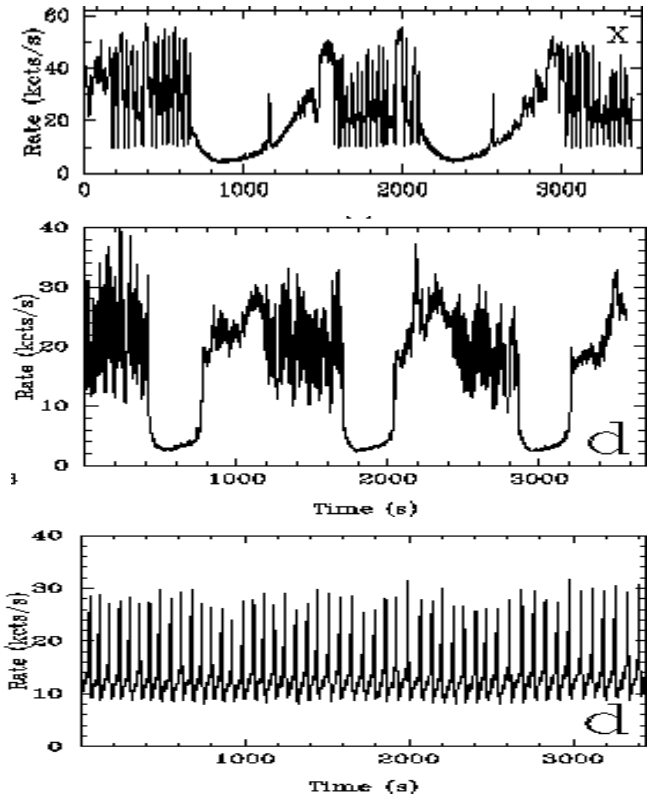

GRS 1915+105 (Strohmayer)

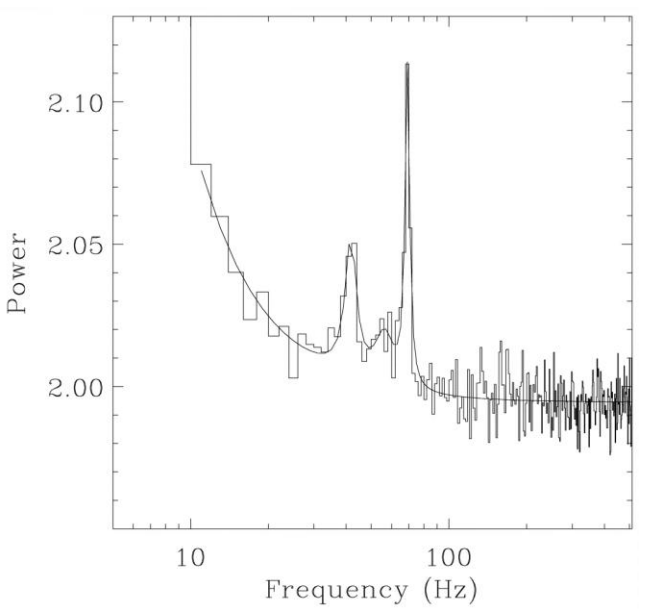

High frequency QPOs (e.g. 40 & 67 Hz repeat in GRS)

Galactic Black Hole Binary (GRB) Cartoon

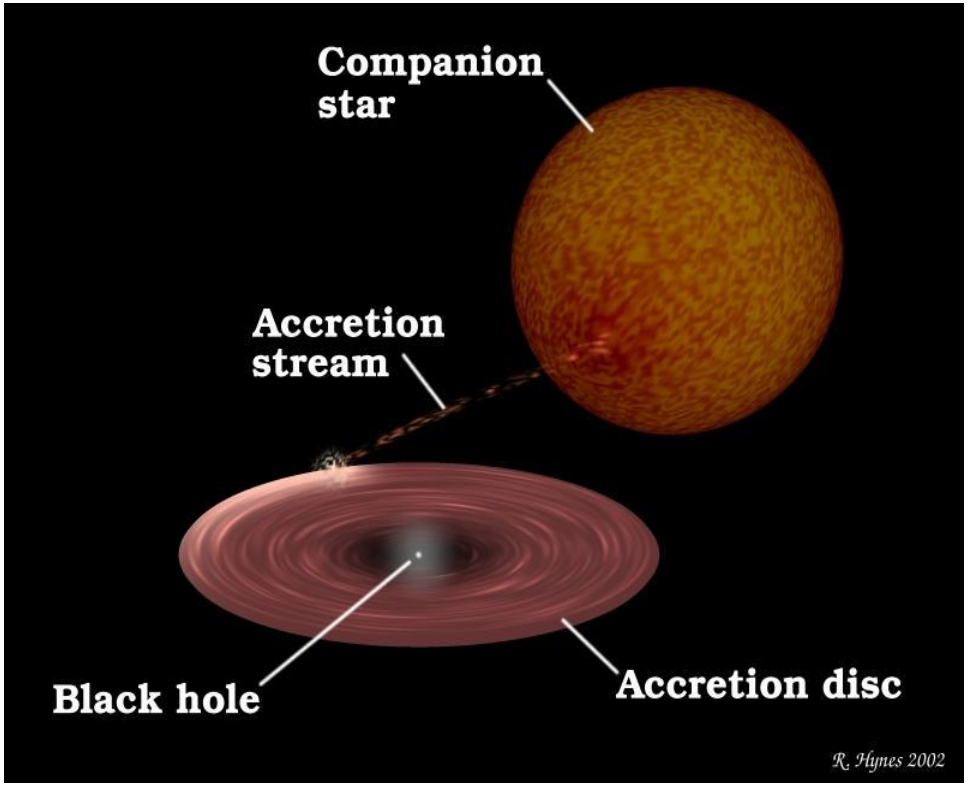

Active Galactic Nuclei (AGN) Cartoon

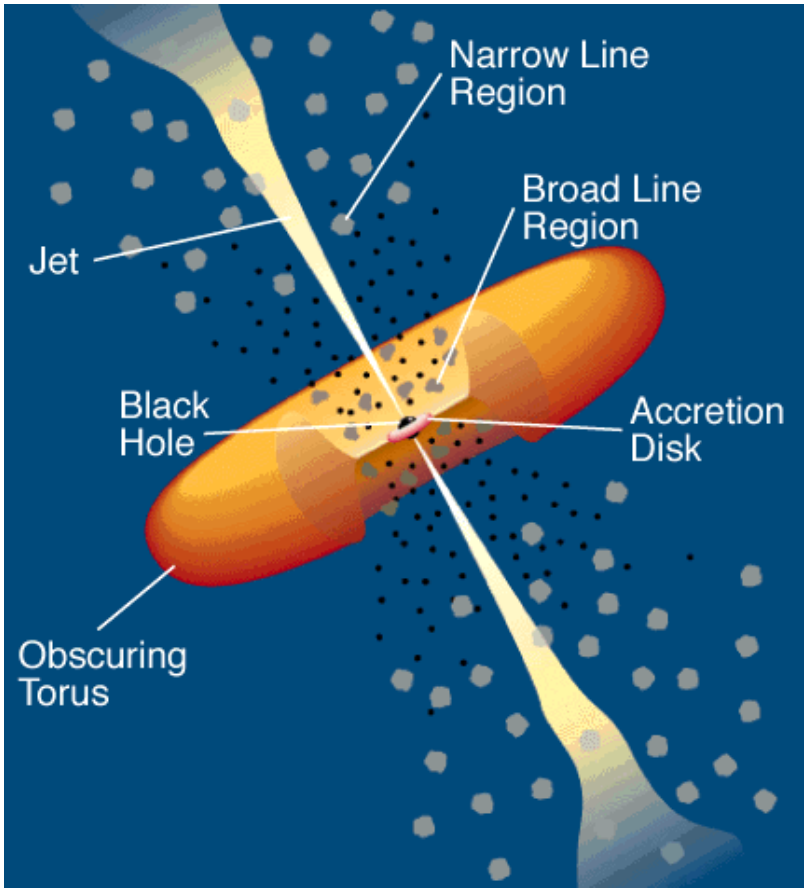

Accretion Disk based emission models,

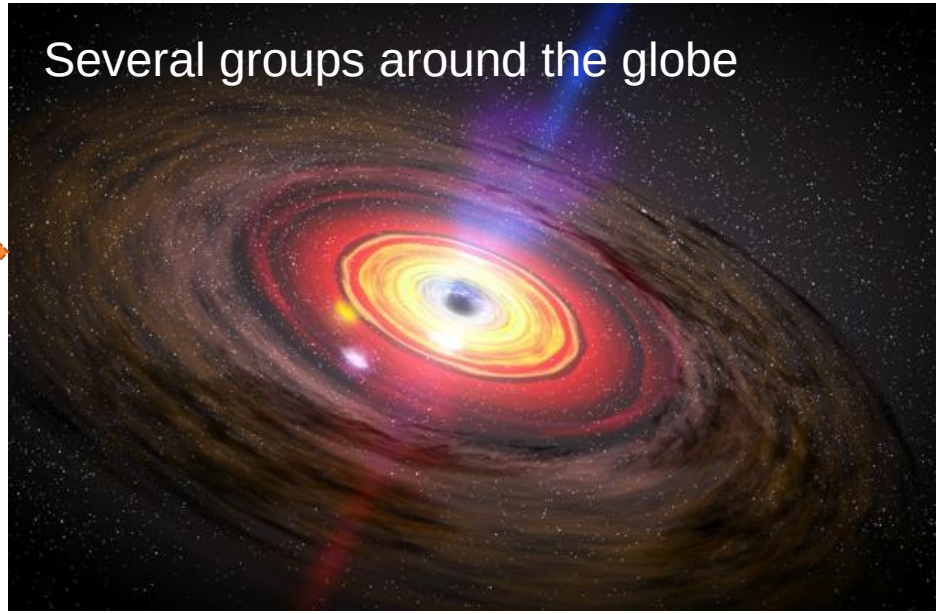

Helical Jet Structure Model

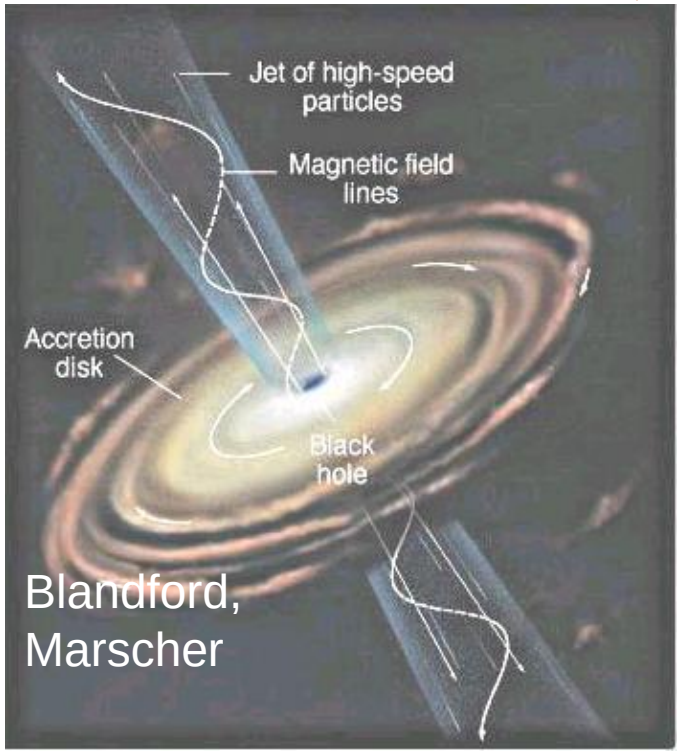

Binary Black Hole Model

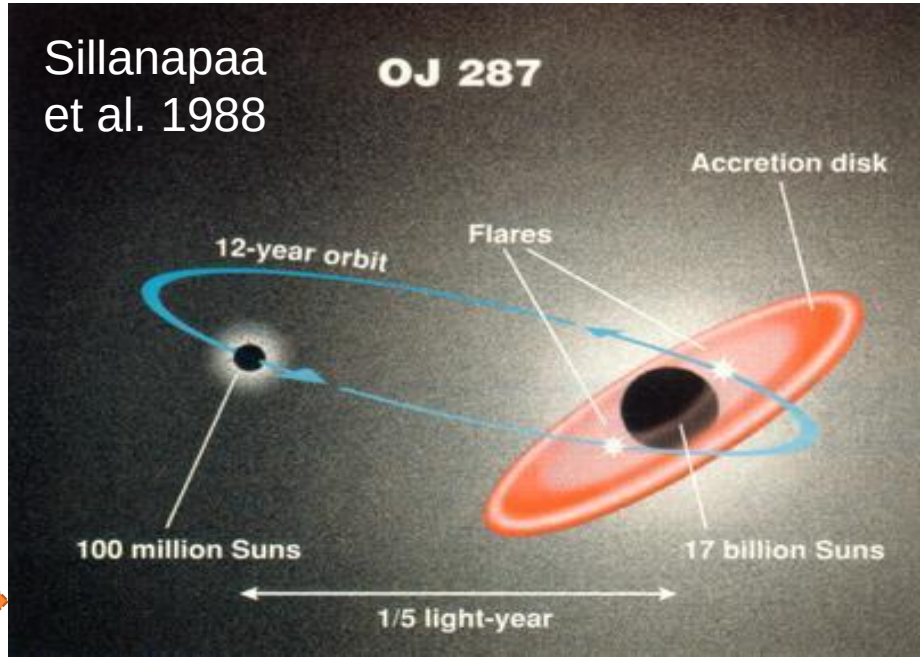

QPOs reported in AGN before 2008

- Fiore, F. et al. 1989, AJ, 347, 171
- Papadakis, I. E & Lawrence, A. 1993, Nature, 361, 233
- Iwasawa, K. et al. 1998, MNRAS, 295, L20

QPOs reported in AGN since 2008

- Espaillat, C. et al. 2008, ApJ, 679, 182
- Graham, et al. 2015, Nature, 518, 74

Later QPO detection in all these papers were either found wrong or statistically not significant

➔ So, search for QPO in AGN should be done very carefully by using multiple techniques.

- QPO in XMM-Newton LC of a narrow line Seyfert 1 galaxy (RE J1034+396) on the timescale of ~ 1h (Gierlinski et al. 2008, Nature) using PSD method.

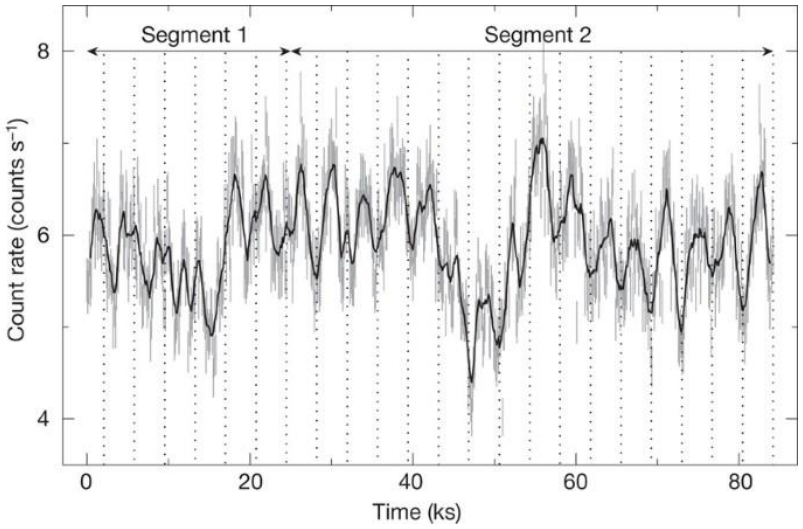

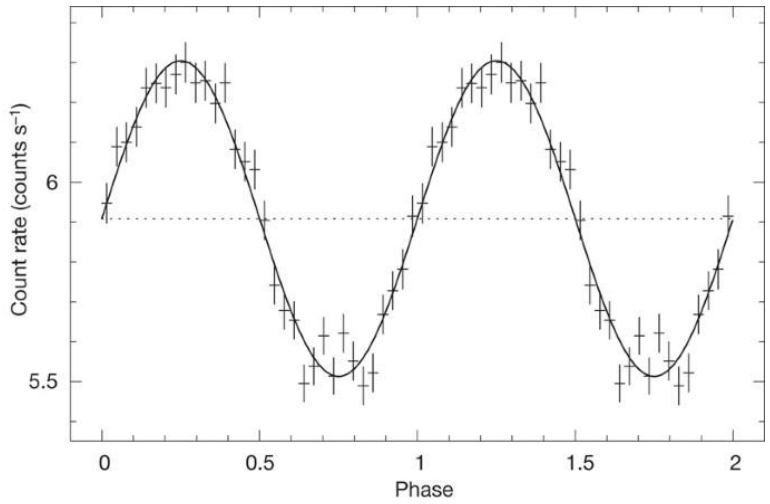

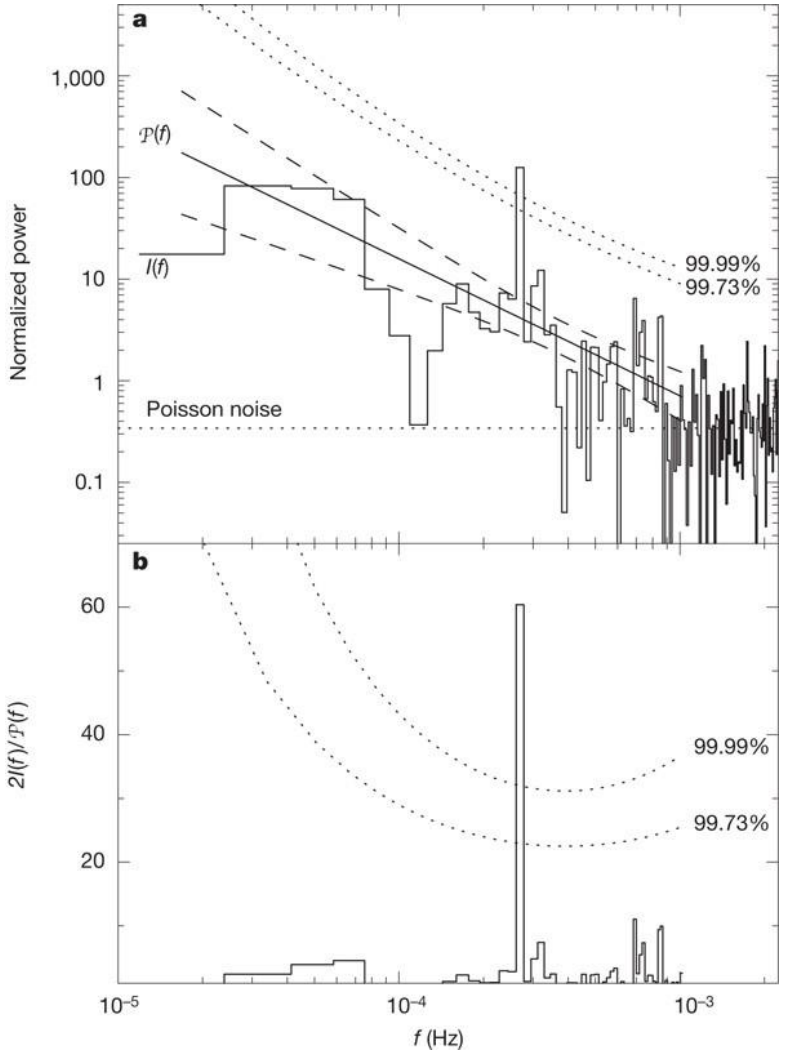

Our Results

EM Band	QPO Results	Time Scale	Methods	Reference
Optical	QPO in S5 0716+714 on 5 occasions	25 to 73 min.	wavelet	ACG, AKS, PJW, ApJ, 690, 216 (2009)
X-ray	QPO in AO 0235+164 QPO in 1ES 2321+419	17 days 420 days	SF, DCF, LSP, Data Folding	BR, PJW, ACG, ApJ, 696, 2170 (2009)
X-ray	QPO in PKS 2155-304	4.6 hour	SF, wavelet, PSD, MHAoV, data folding	PL, ACG, HG, PJW, A&A Lett. 506, L17 (2009)
X-ray	Hint of QPO in ON 231 Hint of QPO in PKS 2155-304	3.3 hour 1.9 hour	SF, PSD	HG, ACG, PJW, ApJ, 718, 279 (2010)
Optical	QPO in S5 0716+714	15 min	SF, PSD, LSP, data folding	BR, ACG, UCJ, SG, PJW, ApJL, 719, L153 (2010)
Optical	Weak QPO in S5 0716+714	1.1 days	SF, PSD, wavelet, MHAoV, data folding	ACG, et al. (34 authors) MNRAS, 425, 2625 (2012)
X-ray	QPO in NLS1 MCG-06-30-15	1 hour	LSP, WWZ (weighted wavelet z-transform)	ACG, et al. (6 authors) A&A Lett., 616, L6 (2018)
Gamma -ray	QPO in B2 1520+31	71 days	LSP, WWZ (weighted wavelet z-transform)	ACG, et al. (6 authors) MNRAS, 484, 5785 (2019)

Our Results

EM Band	QPO Results	Time Scale	Methods	Reference
Optical & Gamma-ray	QPO in CTA 102	7.6 days with 8 cycles	LSP, WWZ, ARIMA	AS, PK, **ACG**, VRC, PJW, **A&A, 642, 129 (2020)**
Gamma-ray	QPO in OJ 287	314 days	LSP, WWZ, ARIMA	PK, AS, **ACG**, AT, PJW, **MNRAS, 499, 653 (2020)**
Optical & Gamma-ray	QPO in 3C 454.3	47 days with 9 cycles	LSP, WWZ, PSD, ARIMA	AS, **ACG**, VRC, PJW, **MNRAS, 501, 50 (2021)**
Radio	QPO in AO 0235+164	965 days	LSP, WWZ, PSD	AT, **ACG**, et al. **MNRAS, 501, 5997 (2021)**
Gamma-rays	Transient QPO in PKS 1510-089	3.6 days & 92 days	GLSP, WWZ, REDFIT, Light curves simulation	**AR et al. 2022, MNRAS, 510, 3641**
Optical	Double peaked QPO in AO 0235+164	8.3 yrs with 2 yrs separation	GLSP, WWZ, REDFIT, Light curves simulations	**AR et al. 2022, MNRAS, 513, 5238**
Optical	QPO in BL Lacertae	13 hours	REDFIT, WWZ, Continuous wavelet transform (CWT)	**SJ et al. 2022, Nature, 609, 265**

Black Hole Mass Estimation with Periodic or QPO Timescale

Causality argument gives the size of emitting region R <= c delta T (obs). Minimum size of such an emitting region is fairly closely related to the gravitational radius of BH,

$$R \geqslant R_g \equiv GM/c^2 \text{ (e.g., Wiita 1985)}$$

The minimum likely period corresponds to the orbital period at the inner edge of the accretion disk, which is usually is given by marginally stable orbit, R_{ms}

For a non rotating (Schwarzschild) BH

$$R_{\rm ms} = 6GM/c^2 = 6R_g$$

a maximal Kerr BH, with angular momentum parameter $a \rightarrow 1$, $R_{\rm ms} \rightarrow R_g$. However, for a more realistic maximum angular momentum parameter of $a = 0.9982$ then $R_{\rm ms} \simeq 1.2R_g$ (e.g., Espaillat et al. 2008).

The angular velocity of co-rotating matter orbiting a BH, as measured by an inertial observer at infinity, is given by (e.g., Lightman et al. 1975)

$$\Omega = \frac{M^{1/2}}{r^{3/2} + a M^{1/2}}, \tag{3}$$

where geometrical units, $G = c = 1$, have been used, and $r = R/R_g$. This leads to an expression for the BH mass in terms of the observed period, P, in seconds,

$$\frac{M}{M_\odot} = \frac{3.23 \times 10^4 P}{(r^{3/2} + a)(1 + z)}. \tag{4}$$

The nominal masses obtained in this fashion for a Schwarzschild BH (with $r = 6$ and $a = 0$) are in Column 7 of Table 1, and those obtained for a maximal Kerr BH (with $r = 1.2$ and $a = 0.9982$) are in Column 8. If the periodic perturbations in the

XMM-Newton data of PKS 2155-304

4.6 hour QPO & 3.8 cycles

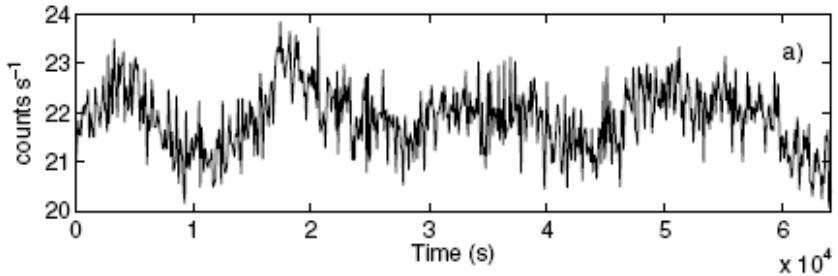

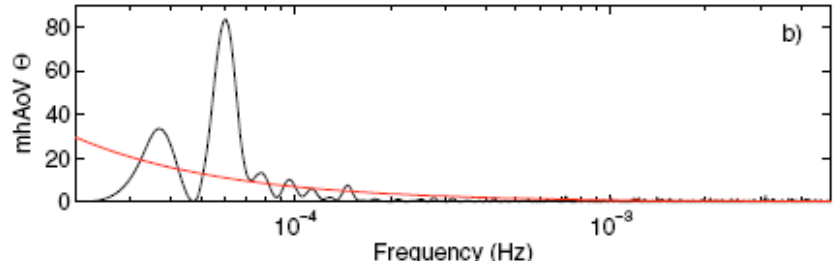

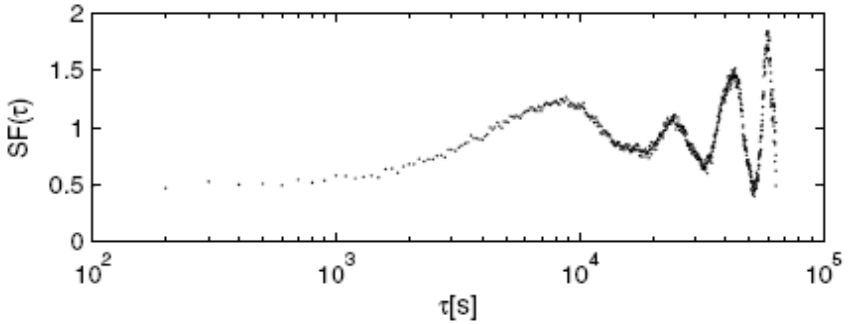

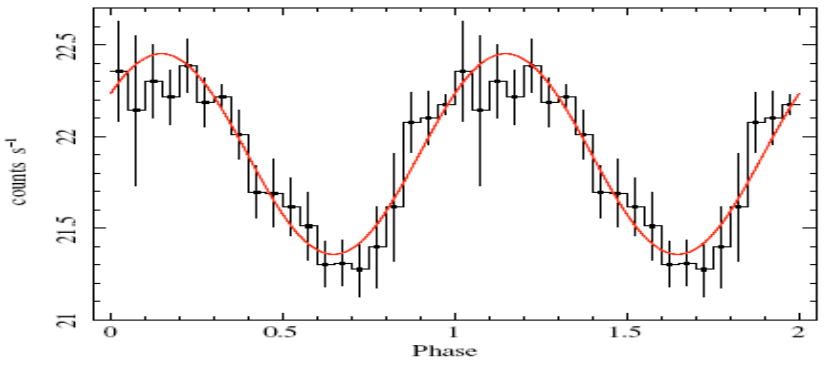

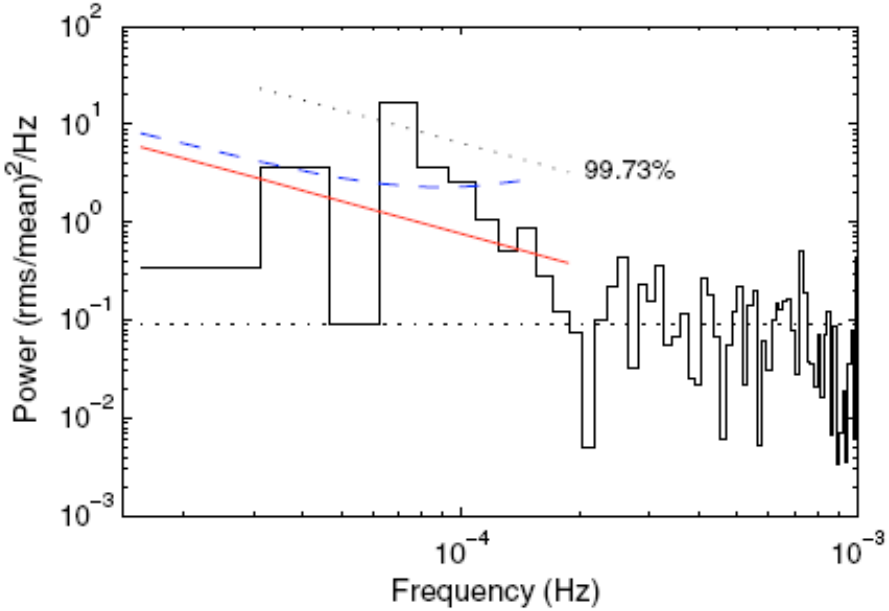

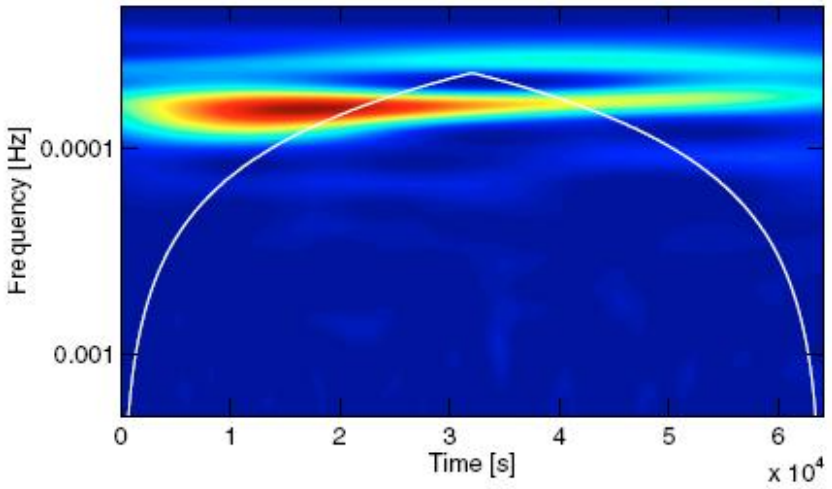

Lachowicz, **Gupta**, Gaur, Wiita, 2009, A&A Lett., **506**, L17

The simplest of these models for BHs would attribute the quasi-periods to particularly strong orbiting hotspots on the disks at, or close to, the innermost stable circular orbit allowed by general relativity (e.g., Abramowicz et al. 1991; Mangalam & Wiita 1993). If such simple models apply in this case, and the QPO is indeed real, then we would estimate the BH mass for PKS 2155−304 to be $3.29 \times 10^7 M$ (Sun) for a non-rotating BH and $2.09 \times 10^8 M$ (Sun) for a maximally rotating BH.

A shock propagating down a jet which contains quasi-helical structures, whether in electron density or magnetic field, can produce a QPO, with successive peaks seen each time the shock meets another twist of the helix at the angle that provides the maximum boosting for the observer (e.g., Camenzind & Krockenberger 1992). Instabilities in jets just might be able to excite such helical modes capable of yielding fluctuations that are observed to occur on the time-scale seen in PKS 2155−304 (e.g., Romero 1995). Or they could arise as the jet plasma is launched in the vicinity of SMBH and thus actually originate in the accretion flow but become amplified in the jet. Another very plausible origin for a short-lived QPO would be turbulence behind the shock in the relativistic jet (e.g. Marscher et al. 1992), as again intrinsically modest fluctuations could be Doppler boosted.

Blazar B2 1520+31

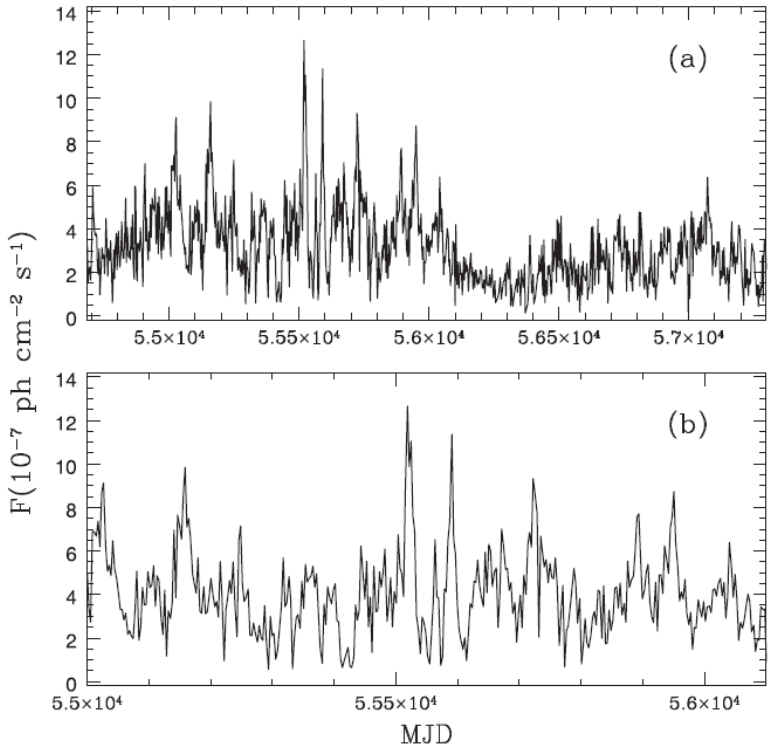

Figure 1. (a) 0.1–300 GeV LAT γ-ray light curve of the blazar B2 1520+31 for data integration times of 3d from 2008 August 5 to 2015 October 5. (b) An expanded segment of the top panel of the light curve taken between 2008 August 5 and 2012 June 22.

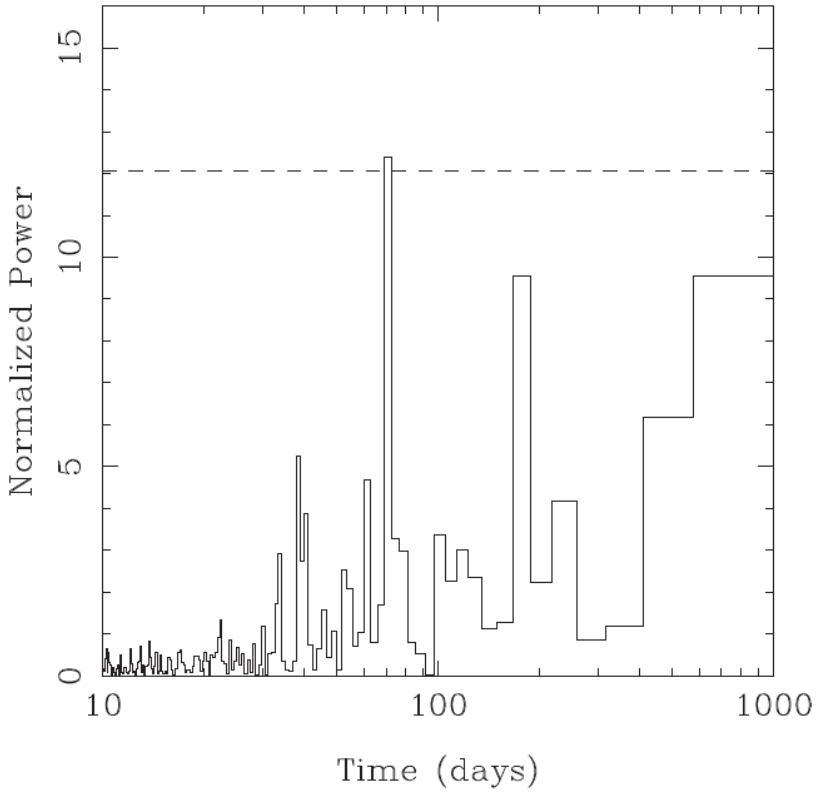

Figure 2. LSP of the light curve in Fig. 1(b). The dashed line represents a null hypothesis or false alarm probability of $p = 0.0001$.

Gupta, et al. 2019, MNRAS, **484**, 5785

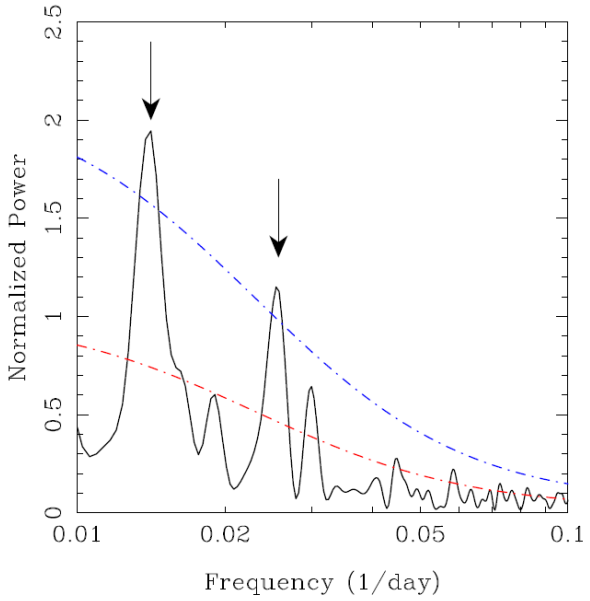

Figure 3. Results of the REDFIT method: the black curve represents the bias-corrected spectra, the red dot–dashed line indicates the computed (AR1) red noise spectrum, and the blue dot–dashed curve shows the 95 per cent χ^2 significance level.

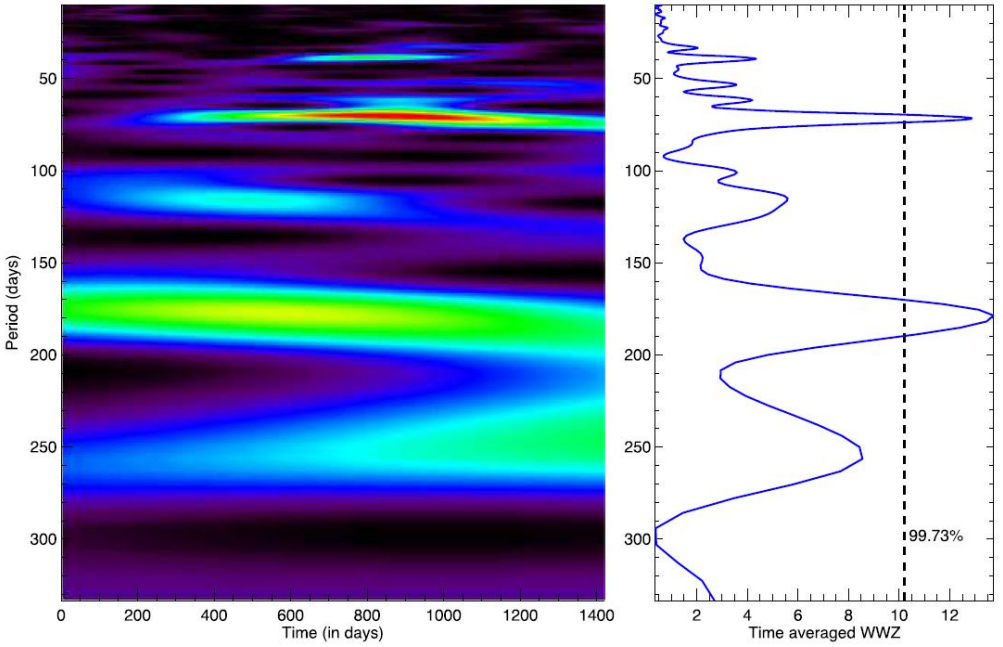

Figure 4. Weighted wavelet Z-transform (WWZ) of the light curve presented in Fig. 1(b). The left-hand panel shows the distribution of colour-scaled WWZ power (with red most intense and black lowest) in the time–period plane; the right-hand panel shows the time-averaged WWZ power (solid blue curve) as a function of period and the 99.73 per cent global significance (dashed black curve).

Fermi data of B2 1520+31

71 days QPO

Estimated BH Mass in the range of 5.4 * 10^9 M_sun (for non-rotating) and 3.4 * 10^10 M_sun (fox maximally rotating) BH

Gupta, et al. 2019, MNRAS, **484**, 5785

3C 454.3

Simultaneous optical and gamma-ray QPO with period of 47 days

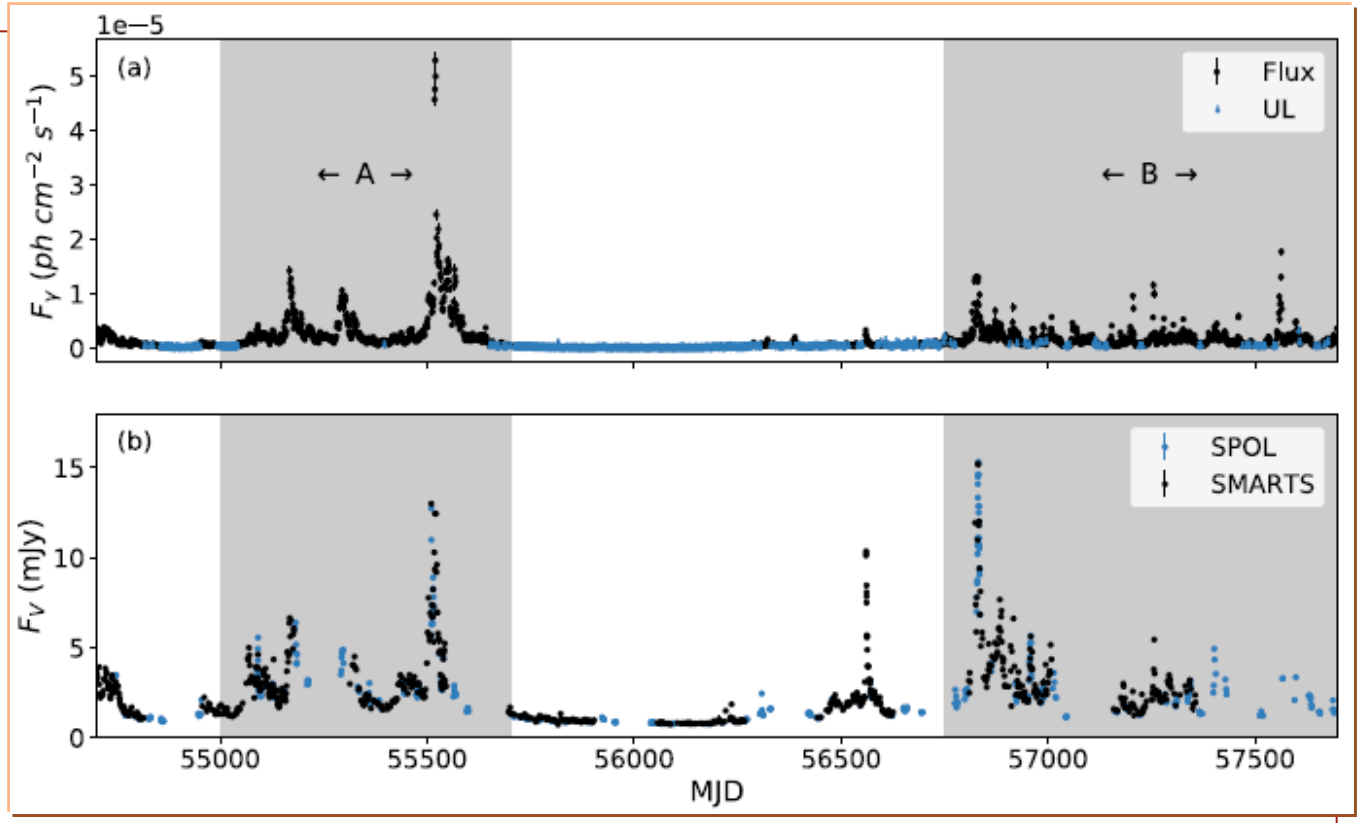

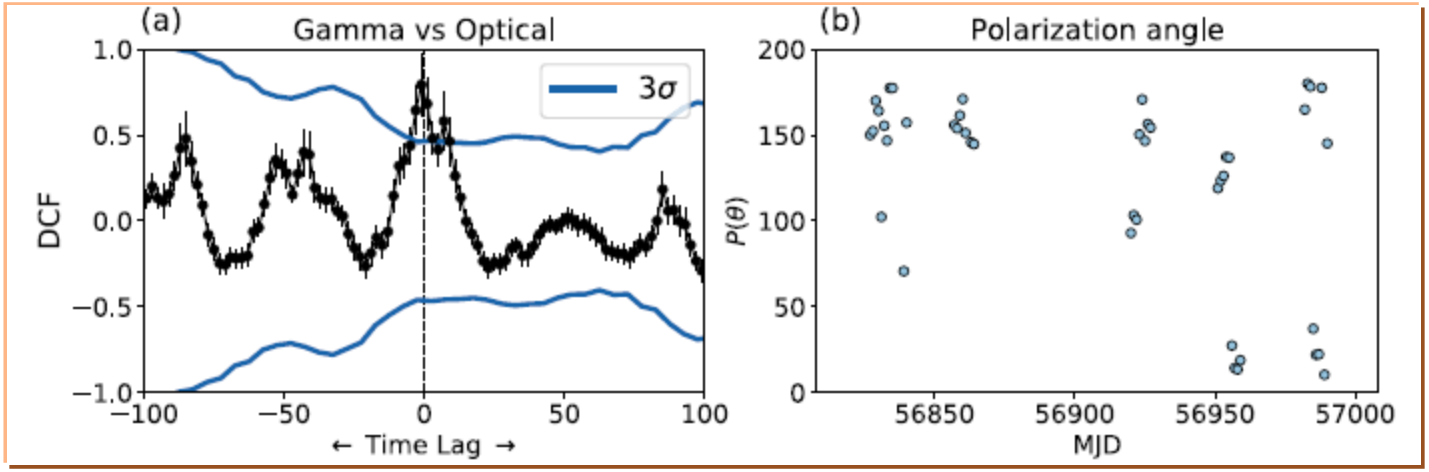

Sarkar et al. 2021, MNRAS, 501, 50

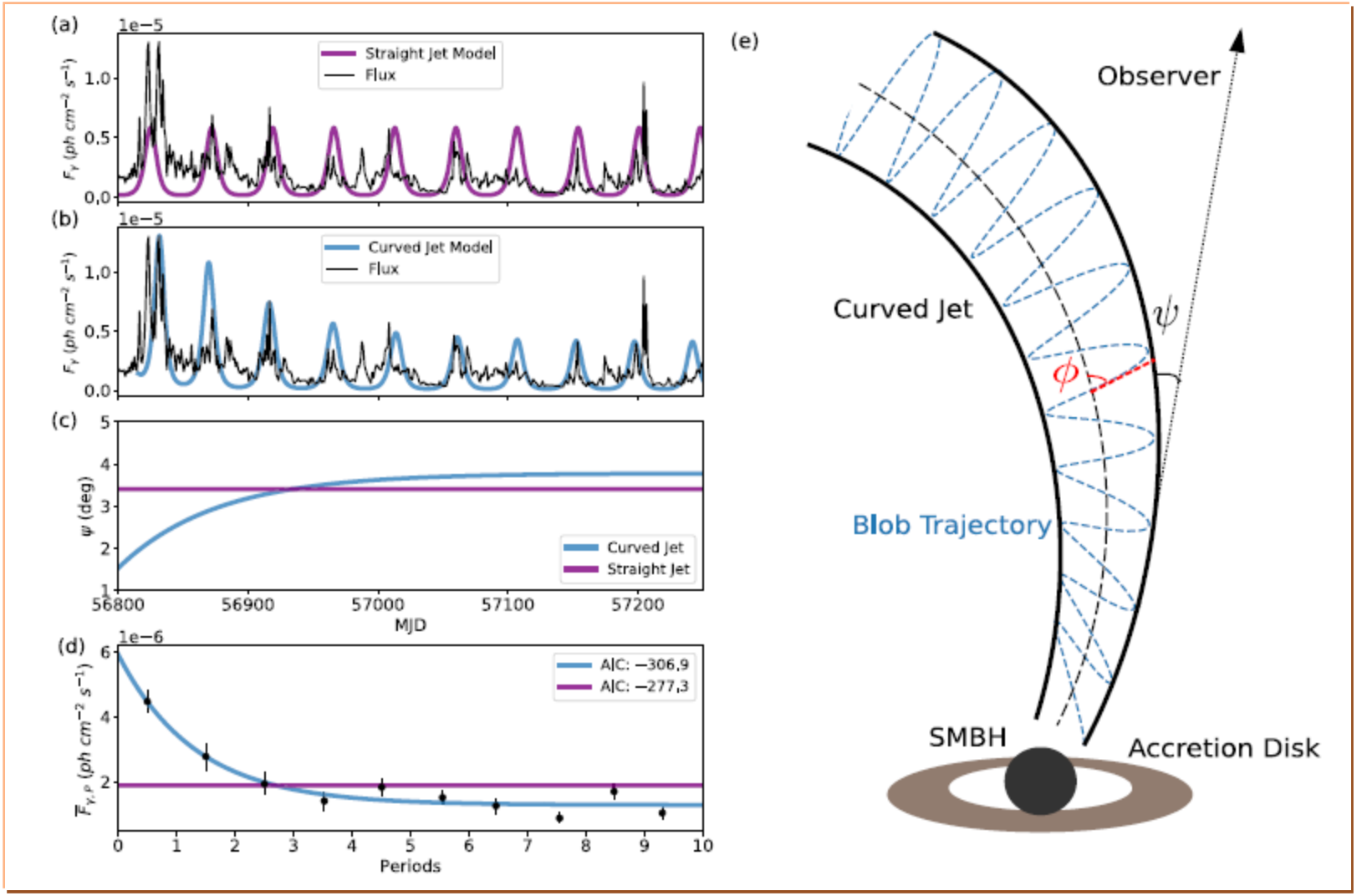

A geometric model involving a plasma blob moving helically inside the curved jet.

Sarkar et al. 2021, MNRAS, 501, 50

PKS 1510 – 089

Fermi-LAT gamma-ray Light curves

3.6 days & 92 days QPOs are detected in two shaded portion of light curves

A geometric model involving a plasma blob moving helically inside the curved jet.

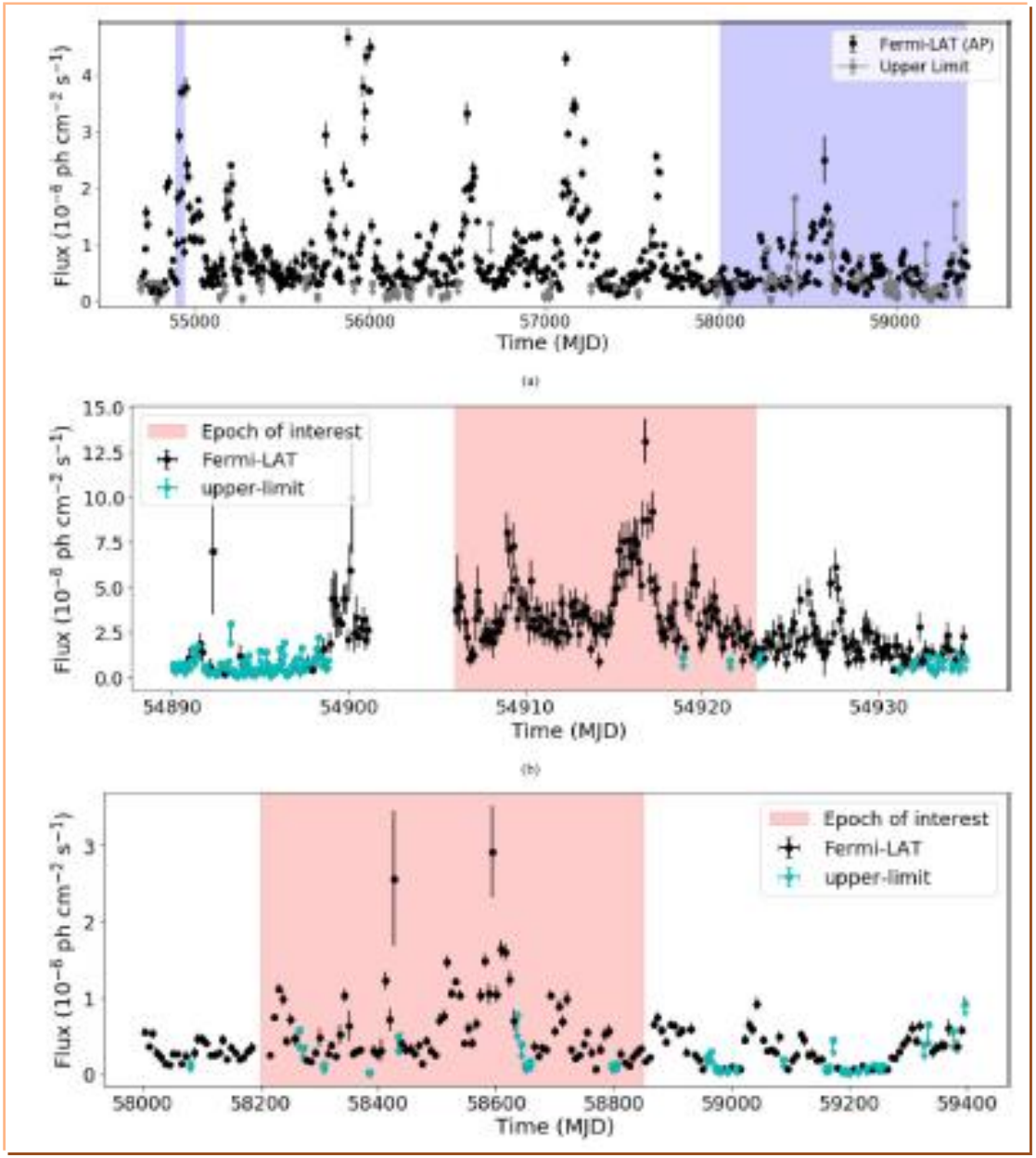

Roy et al. 2022, MNRAS, 510, 3641

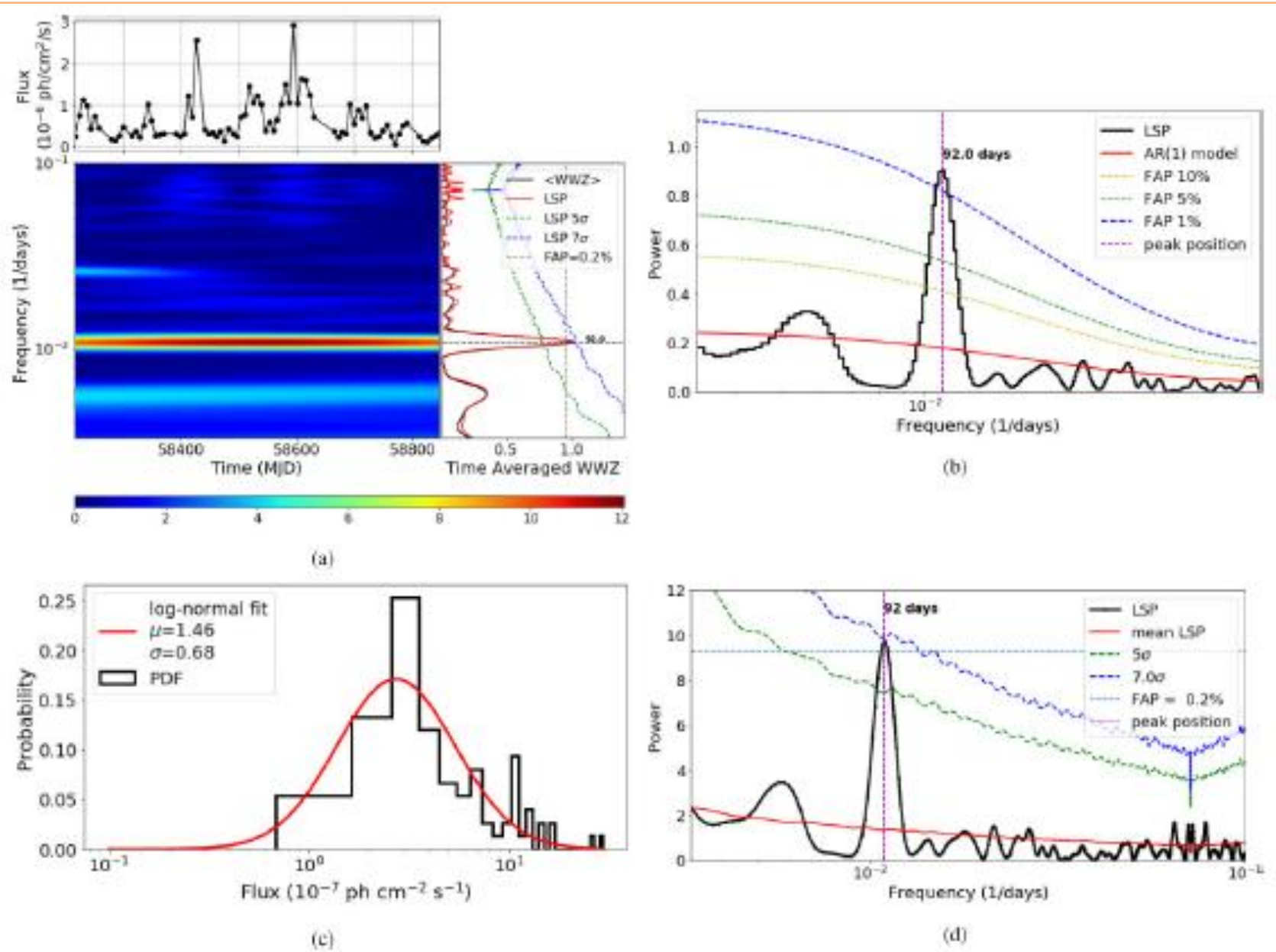

Roy et al. 2022, MNRAS, 510, 3641

Summary

- In a single LC of HBL PKS 2155 – 304, we noticed stable flux, QPO, decline flux and flaring state. Simultaneous Optical, UV and X-ray SEDs are well fitted by PLLP (power-law + log parabolic) model in PKS 2155 – 304.
- In LTV LCs, optical and UV LCs were correlated, and soft and hard X-ray LCs were correlated in 3C 273. We also found, synchrotron cooling and particle acceleration are at work on different epoch of observations.
- Mrk 421 observations with XMM-Newton, Chandra, Suzaku and NuStar show X-ray variation on IDV and STV timescales. NuStar observations show double peaked huge outburst.
- In a multi-wavelength observational campaign of S5 0716+714, IDV is detected optical and radio bands, different optical bands are well correlated, 2.8cm band light curve leads 6cm and 11cm light curves.
- Simultaneous optical, X-ray and gamma-ray light curves of 3C 454.3 show strong correlated variability in optical and gamma-ray in which gamma-ray is leading optical by ~4 days, but X-ray is not correlated.
- Simultaneous multi-wavelength observations of 3C 454.3 show strong flux variation in NIR, optical, X-ray and gamma-rays which was anti-correlated with optical polarization and polarization angle.
- We detected FeKα line near its rest energy 6.4 keV in one of the observation of 3C 273.
- QPOs in Blazars are rare but occasionally detected on diverse timescales.

I thankfully acknowledge my several Ph.D. and postdoctoral students, and large number of collaborators all around the globe including Evgeni Semkov, Rumen Bachev, Anton Strigachev, Goran Damljanovic, Oliver Vinece, and several other team members from Bulgaria and Serbia for the collaborative work.

THANKS